OAK RIDGE NATIONAL LABORATORY
MANAGED BY UT-BATTELLE FOR THE DEPARTMENT OF ENERGY

ORNL/TM – 2012/506

FINAL REPORT

Investigation of Surface Treatments to Improve the Friction and Wear of Titanium Alloys for Diesel Engine Components

Peter J. Blau, Kevin M. Cooley, and Melanie J. Kirkham
Oak Ridge National Laboratory

with

Dinesh G. Bansal
Oak Ridge Associated Universities

Prepared by
Oak Ridge National Laboratory
Oak Ridge, TN 37831
Managed by
UT-BATTELE, LLC
for the
U.S. Department of Energy
Under contract DE-AC05-00PR2225

September 30, 2012

Approved for
Unlimited Distribution

UT-BATTELLE

Investigation of Surface Treatments to Improve the Friction and Wear of Titanium Alloys for Diesel Engine Components

Peter Blau, Kevin M. Cooley, and Melanie Kirkham
Oak Ridge National Laboratory

and

Dinesh G. Bansal
Oak Ridge Associated Universities*

prepared for the

U.S. Department of Energy
Office of Energy Efficiency and Renewable Energy
Propulsion Materials Program

*currently Cummins Inc., Technical Center, Columbus, Indiana

Foreword

This final report summarizes experimental and analytical work performed under an agreement between the U.S. Department of Energy, Office of Energy Efficiency and Renewable Energy, Office of Transportation Technologies, and UT-Battelle LLC. The project was directed by Jerry Gibbs, of the U.S. Department of Energy's Propulsion Materials Program, with management by D. P. Stinton and J. A. Haynes of ORNL. Participants included Peter J. Blau (Principal Investigator), Kevin M. Cooley (senior technician), Melanie J. Kirkham (materials scientist) of the Materials Science and Technology Division or ORNL, and Dinesh G. Bansal, a post doctoral fellow employed by Oak Ridge Associated Universities (ORAU) and who, at the time of this writing, is an engineer with Cummins, Inc.

This report covers a three-year effort that involved two stages. In the first stage, and after a review of the literature and discussions with surface treatment experts, a series of candidate alloys and surface treatments for titanium alloy (Ti-6Al-4V) was selected for initial screening. After pre-screening using an ASTM standard test method, the more promising surface treatments were tested in Phase 2 using a variable loading apparatus that was designed and built to simulate the changing load patterns in a typical connecting rod bearing. Information on load profiles from the literature was supplemented with the help of T.C. Chen and Howard Savage of Cummins, Inc. Considering the dynamic and evolving nature of materials technology, this report presents a snapshot of commercial and experimental bearing surface technologies for titanium alloys that were available during the period of this work. Undoubtedly, further improvements in surface engineering methods for titanium will evolve.

The authors gratefully acknowledge the following individuals and companies who provided surface treatments, material suggestions, or coatings for study at nominal or no charge:

Jason Goldsmith, Greenleaf Inc.
O. L. Eryilmaz, Argonne National Laboratory
Gary Wittman, Tiodize Technologies
Al Segall, Pennsylvania State University
Don Jordan, Solar Atmospheres

Clifton Higdon , Eaton Corp.
Dave Bell, Phygen Coatings, Inc.
Dave Breuer, Metal Improvement Co.
Christopher DellCorte, NASA
John Colegrove, Ellison Surface Technologies

No proprietary information has been included in this report.

Peter J. Blau
Oak Ridge National Laboratory
September 2012

CONTENTS

1.0 Executive Summary

The fuel efficiency of ground vehicles, like heavy trucks, can be improved by reducing their weight, minimizing internal friction losses, improving aerodynamics, and lowering rolling resistance with advanced tires. The current effort addresses lowering both engine component weight and friction losses. While primarily developed for aerospace structures, titanium alloy Ti-6Al-4V has the potential to replace heavier steel and cast iron in friction and wear-critical diesel engine components like connecting rods, movable turbocharger vanes, pistons, and even crankshafts. While Ti-6Al-4V exhibits excellent corrosion resistance, good fatigue strength, and satisfactory fracture toughness, it has poor friction and wear characteristics. Thanks to the aerospace industry's interest in reducing fretting wear in turbine engines, a variety of approaches are available to improve the friction and wear of Ti contact surfaces. Unfortunately, the majority of these are impractical for diesel engine connecting rod bearings because such surfaces must withstand well over a billion lifetime sliding contact cycles and be compatible with conventional lubricants. Using conventional inserts like plated bronze for big end bearings in Ti alloy connecting rods is a lower-risk, near-term solution to light-weighting engines, but some bronzes contain lead, a material with negative environmental impact. The current project investigated whether a Ti alloy could be surface engineered to avoid the need for inserts, and in addition, extend its possible use to other bearing-critical surfaces in the engine like cam lobes which also experience moving contact.

A two phase effort was conducted. During Phase 1, more than twenty surface engineering processes were compared in engine-conditioned diesel oil in a reciprocating pin-on-flat (RPOF) apparatus (ASTM Standard G133). Candidate treatments included diffusion treatments (carburizing, nitriding, oxidizing), the application of hard coatings (TiN, CrN, diamond film), application of a plated coating used on actual bearing inserts (Cu-Ni-In), a Ti-matrix TiB_2 in situ-formed composite, and mechanical working (by shot peening or hammer planishing). In addition to studying the effects of individual surface treatments, some treatments were combined in an attempt to discover possible synergistic benefits. X-ray studies indicated that subsurface microstrain levels varied depending on the combination of treatments. Of the initial set tested in Phase 1, five promising treatments were down-selected for further investigation in Phase 2.

A variable-loading bearing tester (VLBT) was designed and built. Programmed to simulate the time-varying load spectrum of a typical connecting rod, the VLBT was used during Phase 2 to compare the frictional behavior and durability of promising surface engineering treatments under the range of lubrication regimes that are typical of engine connecting rod bearings. The treatments down-selected in Phase 1 did not produce the same rankings when they were tested using the VLBT because it used a different contact geometry, unidirectional motion, and higher speed than the Phase 1 procedure. VLBT data were more typical of the mixed or hydrodynamic lubrication regimes than were the RPOF data which typified boundary lubrication conditions. Implications for these results for applications like connecting rod bearings are discussed. The RPOF test of Phase 1 stressed the materials more than did the VLBT test of Phase 2 which operated under nearly full-film lubrication. In fact, some treatments that failed to pass Phase 1 criteria, but were added to the test matrix for comparison, ranked higher under VLBT conditions. Clearly, test methodology can emphasize either material characteristics or lubrication characteristics. As a result, different tests produce different friction and wear rankings for the same set of sliding partners.

Results of Phase 1 were published in the proceedings of the 18th International Conference on Wear of Materials, and results from Phase 2 have been accepted for the 19th International Conference on Wear of Materials (2 separate papers). These data support a series of recommendations for diesel engine designers interested in light alloys.

A key finding from the current work is that most of the coatings and surface treatments employed here affect only a few thousandths of an inch (small fractions of a millimeter) deep in the bearing surface, and once this thin zone in worn through, the exposed Ti substrate exhibits poor friction and wear behavior. In addition, such treatments tend not to be self-healing or easily restorable; therefore, there is little alternative but to replace the entire part (or machine it out and add inserts). Based on current results, two surface engineering treatments offered the best combination of resistance to material contact effects (Phase 1 tests) and performance under well-lubricated conditions (Phase 2 tests). The first was the commercial chromium nitride (CrN) coating known as FortiPhy™, and the second was an experimental high velocity powder consolidated (HVPC) coating from Pennsylvania State University containing Ni with a B additive. The latter choice was based on its ranking during lubricated friction and wear results.

In summary, one conservative approach to the use of Ti in friction and wear-critical engine components is simply to avoid the use of bare or treated Ti surfaces entirely, and use inserts of traditional bearing materials. The case in point is for lightweight connecting rods, but in other cases, the results of the current work suggest a potential for the use of surface treated or thin layer coated titanium alloys in components that operate under mixed film or thick film lubrication conditions where resistance to solid/solid moving contact is less of an issue.

2.0 Statement of Objectives

The overall goal of this effort is to facilitate a 50% increase in heavy vehicle freight efficiency (ton-miles per gallon). To support this goal, there is an effort to increase the use of lightweight structural materials, like Ti-based alloys, in certain engine components which require low friction while also resisting wear. Since bare Ti is unacceptable for bearing surfaces, the solution will require surface engineering treatments or coatings. The current effort focuses on identifying the most promising ones, be they experimental or commercialized.

The objective of this effort is to provide guidance to diesel engine designers for how titanium-based alloys could, by virtue of advanced surface engineering practices or coatings, be used for engine components that require low friction surfaces and high wear resistance. The large end bearing on a connecting rod is a particular focus of this work, but other potential applications include exhaust gas recirculation valves, tappets, valves and valve guides, crankshafts, and piston skirts. The ultimate purpose is to anticipate future needs for lightweight materials like titanium so that the diesel industry's introduction of new technology can be accelerated.

3.0 Benefits to the DOE Office of Transportation Technologies Mission

The introduction of advanced materials into transportation has historically taken from 5-20 years, depending on the maturity of the technology, the urgency of the need for property improvement or cost control, the ability or inability of current materials to meet design requirements for performance and durability. The greater the engineering drivers, the shorter the material introduction cycle, especially if current materials do not suffice. A great deal of federal investment has been made in lightweight materials technologies for transportation, material classes have included metals, ceramics, and composites based on a wide variety of matrix materials. Some of these materials have been commercialized and others with encouraging performance characteristics still wait in the wings, pending cost reduction. Relative to steels and cast irons, the density of metals like titanium, aluminum, and magnesium offer potential weight savings if properly employed in engine and drivetrain components. For example, ORNL has previously published assessments of the use of titanium alloys for heavy truck brakes [1,2]. As with any commercial material technology, there must be a trade-off between performance and cost. Sometimes, the need to meet industry regulatory requirements overrides cost penalties.

4.0 Technical Introduction, Approach, and Results of Experimental Work

4.1 Introduction and Approach

While Ti alloys have been successfully employed in a wide variety of structural applications – from aircraft* and submarine components to high-end sports equipment and biomedical implants – Ti alloys have not been widely used in ground transportation components. Among the main reasons for its relative scarcity in automobiles and trucks has been material cost and availability in an industry in which a few pennies per vehicle can influence material selection. The cost penalty for Ti could be off-set if (a) raw material and manufacturing costs were decreased, and (b) the performance and fuel efficiency benefits of Ti alloys' light weight, specific stiffness, and corrosion resistance off-set its cost.

Like aerospace components and sports equipment, heavy vehicle engines and drive trains could be light-weighted using Ti, but there is an additional problem to be considered. Namely, Ti alloys, like other light alloys based on Al and Mg, suffer from a lack of good friction and wear characteristics and that make use in bearings, gears, and other kinds of moving surface contacts problematic. However, the technical community has not quite given up on Ti for bearing surfaces and in fact has invested considerable effort in surface engineering Ti alloys using coatings and various kinds of diffusion treatments. Much of this work has been focused on aerospace applications – notably fretting of Ti in aircraft turbine engine blades and discs. Relatively little work has been aimed at other kinds of wear parts and types of wear in lubricated situations. Specific surface-critical applications include piston/cylinder contact surfaces, roller followers, crank shafts, valve guides, valve seats, and connecting rods. The latter application is the focus of the current work, whose intent is to identify promising approaches to improve the surface durability and lubricity of Ti alloys.

The parts and features of a typical diesel engine connecting rod are shown in Figure 1. A diesel engine connecting rod from a commercial diesel engine is also shown in Figure 2. There are two primary bearings. The upper, small end bearing experiences reciprocating sliding between the bearing and wrist pin as the piston oscillates, while the big-end bearing experiences continual motion in one direction.

Bearing Materials. The design of most connecting rod bearings involves the use of inserts. In order to provide a combination of stiffness, running-in performance and lubricity, such inserts are often composed of a number of layers and platings, depending on the engine manufacturer [3]. Copper-based alloys (bronzes), like those listed in Table 1, have historically been used connecting rod bearings [4]. Note that many of them contain lead (Pb), making recycling or wear debris for such materials a concern for environmental reasons. It would be desirable to use Ti alloy other than a leaded bronze for that reason, if such bearings could be made to work.

(* Each Boeing 787 aircraft contains as much as 100 tons of Ti-alloys. See: www.commoditymarketing.com.au /**titanium**.php.)

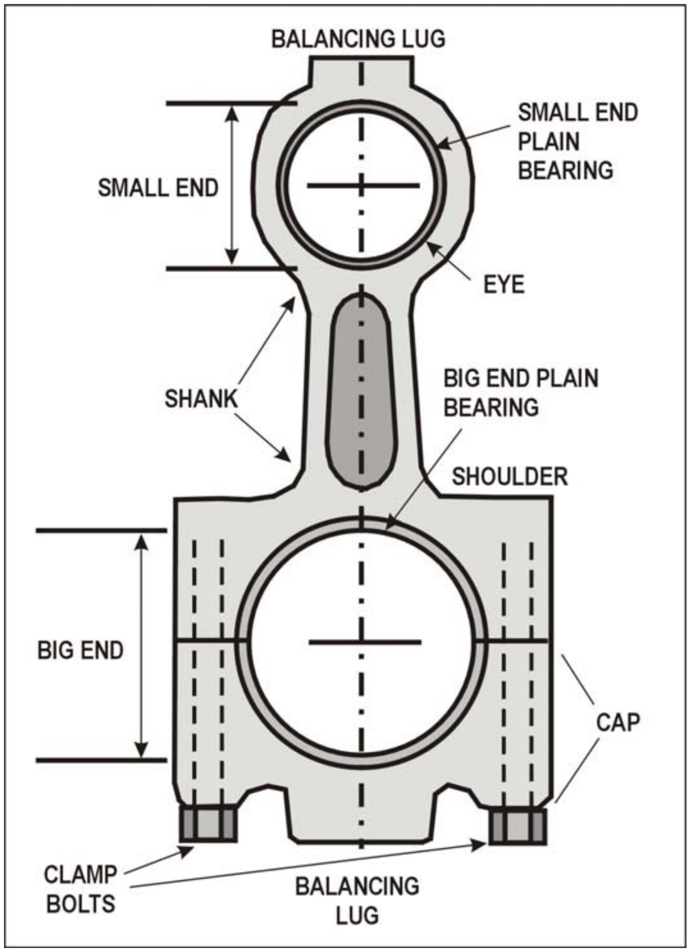

Figure 1. Parts of a typical connecting rod.

Figure 2. Commercial diesel engine connecting rod.

Table 1.
Bearing and Bushing Alloys used for Connecting Rods
(Adapted from ref [4], Table 11-11.)

Category	Designation	Composition
Aluminum-based	SAE 770	6.25 Sn, 1 Cu, 1, Ni, bal. Al
	SAE 780	6 Sn, 1, Cu, 1.5 Si, 0.5 Ni, bal. Al.
	SAE 781	4 Si, 1 Cd, bal. Al
Copper-based	SAE 48	70 Cu, 30 Pb
	SAE 49	76 Cu, 24 Pb
	SAE 480	65 Cu, 35 Pb
	SAE 481	60 Cu, 40 Pb
Tin-based	SAE 11*	87.5 Sn, 6.75 Sb, 5.75 Cu
	SAE 12*	89 Sn, 7.5 Sb, 3.5 Cu
Lead-based	SAE 13*	6 Sn, 10, Sb, bal. Pb
	SAE 14*	10 Sn, 15 Sb, bal. Pb
	SAE 15*	15 Sb, 1 Sn, 1 As, bal. Pb

*Note: 'Babbitt' alloy. Babbitt alloys comprise more than one composition, and are intended to serve as bearing materials. They are mixtures of Cu, Sn, Pb, and Sb. They were named eponymously after Isaac Babbitt who invented them in the early 1800s.

A cross section of a commercially insert for a big end bearing is shown in Figure 3. The top layer is a thin plated coating of about ~ 11-12 μm in thickness. Below it is a bronze layer of thickness ~ 248-250 μm, and below that (blue in the image) is the steel backing plate. The light and dark gray phases in the interdendritic areas of the bronze are Pb that is added for lubricity.

Knoop microindentation hardness data for of the various layers shown in Figure 3 are given in Table 2. Note that there is a factor of about 10 in hardness difference between the soft upper plating and the backing plate, with a bronze layer having intermediate hardness. The soft plating tends to wear off during the running-in period and expose the underlayer for the rest of the service lifetime. Running-in, when done properly establishes the surface conditions for successful long-term operation.

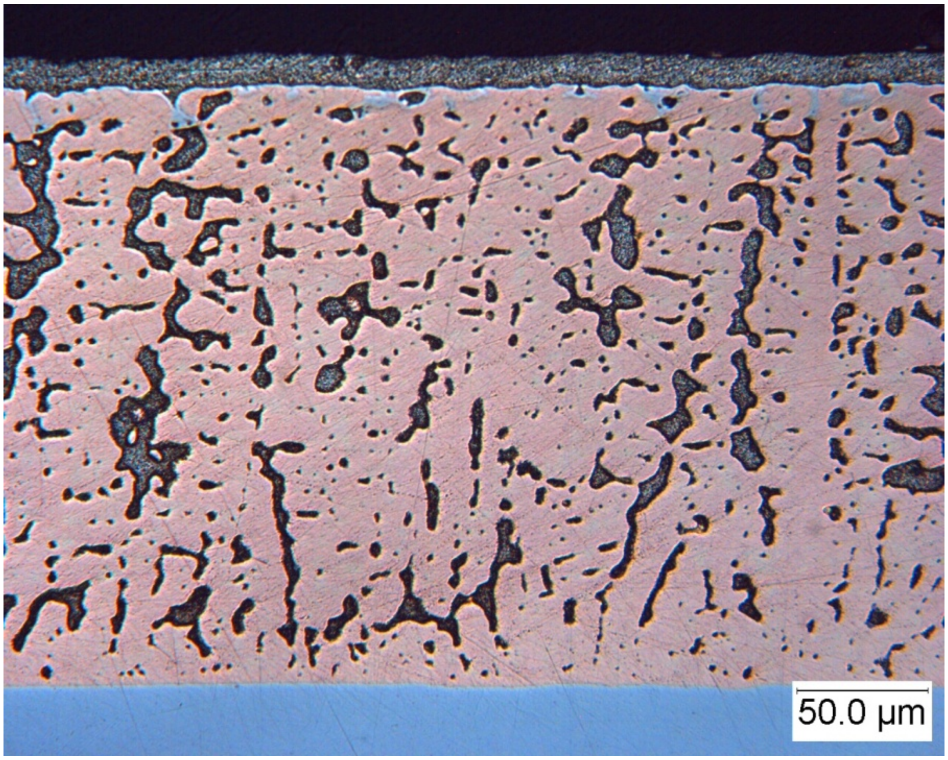

Figure 3. Polished cross-section of a large end bearing insert (polarized light).

Table 2. Knoop Microindentation Hardness of Layers in a Bearing Insert

Material	**Test Load** (g-f)	**HK, average** (kg/mm^2)	**HK, average** (GPa)
Steel backing	10	215.1	2.11
	25	230.4	2.26
	100	219.7	2.16
Bronze, matrix phase	10	107.9	1.06
	25	114.1	1.12
Top coating layer	10	28.2	0.28

Crankshaft Materials. The friction and wear of a plain bearing or bushing depends upon the successful mating of opposing materials. In the current case, the engine crankshaft rotates inside each connecting rod bearing. Several kinds of forged and heat-treated steels are commonly used (see Table 3). The choice of the crankshaft material is dictated by engine-specific characteristics, cost, availability, machinability, and other engineering factors.

Table 3.
Typical Crank Shaft Alloys
(Compositions given in weight %, Source: [5])

Alloy Type	Composition / Description	Approximate Hardness
Mn-Mo steel	Composition: 0.38 C, 1.5 Mn, 0.3 Mo. Forged, oil quenched and tempered. Compatible with bearings plated with Al-Sn or Cu-Pb	250 Brinell
1%-Cr-Mo Steel	Composition:0.4 C, 1.2 Cr, 0.3 Mo. Forged, oil quenched and tempered. Can be flame or induction hardened in addition. For highest hardness, can be nitrided. Compatible with bearings plated with Al-Sn or bronze.	280-480 Brinell
2.5%-Ni-Cr-Mo Steel	Composition: 0.31C, 2.5 Ni, 0.65 Cr, 0.55 Mo. Forged, oil quenched and tempered. Favored in heavy duty diesels.	300 Brinell
3%-Cr-Mo or 1.5%-Cr-Al-Mo Steel	Compositions: (a) 0.15 C, 3 Cr, 0.5 Mo; (b) 0.3 C, 1.5 Cr, 1.1 Al, 0.2 Mo. Oil quenched and tempered. The shafts are also case-hardened by nitriding. Favored in heavy duty diesels.	(a) 800-900 HV (b) 1050-1100 HV
Nodular cast irons	Composition: 3 – 4 C, 1.8 - 2.8 Si, with graphite nodules dispersed in a pearlite matrix. Ce or Mg are used to achieve this structure Flame or induction hardening are used to increase surface hardness.	550-580 Brinell

In the present work, we chose a readily available alloy steel 8620 with an as-received hardness of about 223 Brinell. Its typical composition is as follows (wt%): 0.18-0.23 C, 0.4-0.6 Cr, 0.7-0.9 Mn, 0.15-0.25 Mo, 0.4-0.7 Ni, and was felt to be sufficiently close in composition to the steels in Table 2 to use as a counterface material.

Lubrication Regimes. In order to evaluate a series of candidate materials and surface treatment for application to a large end connecting rod bearing in a laboratory, it is important to understand the operating environment and introduce similar variables for screening. In the current case, we focused on relative motions in the contact and the variations in load that occur as such a bearing rotates. It was established by the work of Martens, Stribeck, and others (as described in [6,7]) that there exists a relationship between the normal force (P), lubricant viscosity (η), and relative velocity (v) of moving bearing surfaces given simple geometries of contact such as a bearing rotating in a journal. That work evolved into a powerful bearing design and analysis tool that is popularly known as the Stribeck curve (shown schematically in Figure 4). In bearing situations like connecting rods in which non-constant loads or speeds might occur, the operating point in the tribosystem in essence travels up or down the Stribeck curve, producing changes in the amount of surface contact, with more solid/solid contact being associated with higher wear and friction levels (up and to the left), and less contact being associated with the development of a thick lubricating film between opposing surfaces (at the bottom of the curve and to the right).

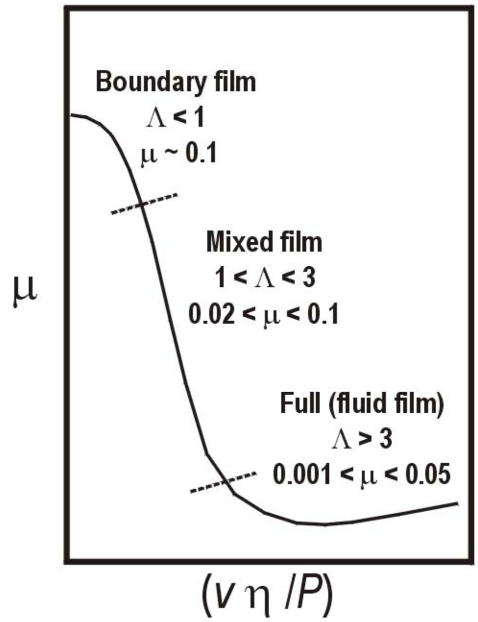

Figure 4. Portion of the Stribeck curve showing various regimes of friction and film thickness.

During the lifetime of a typical diesel engine, connecting rod bearing housings typically sustain as many as a billion or more stress cycles, ranging from the high compressive forces due to combustion and high tensile forces due to inertia [8].

The changing loads due to rotation of a connecting rod bearing in an automobile engine was reported by Taylor [9] in the form of a polar diagram in which bearing load is plotted as a function of the angle of rotation, with two full strokes equaling a single compression, combustion, and exhaust cycle. Such a curve was replotted in linear rather than polar formal in Figure 5. The relative changes in load with time served as a guide to programming the forces on the apparatus which is described later in this report.

The typical magnitude of the film thickness ratio (Λ), defined as the dimensionless ratio of lubricant film thickness to composite roughness, is also associated with certain lubrication regimes, as in Figure 4. It can be assumed that the farther up and to the left one travels on the curve, the more frequent and intense is the surface contact, with very little contact occurring in the mixed film region and more in the boundary film region. Thus, as operating conditions for a transient tribo-contact like an engine bearing or piston on liner change during the course of operation, the degree of solid contact and the probability of wear at any instant of time also vary.

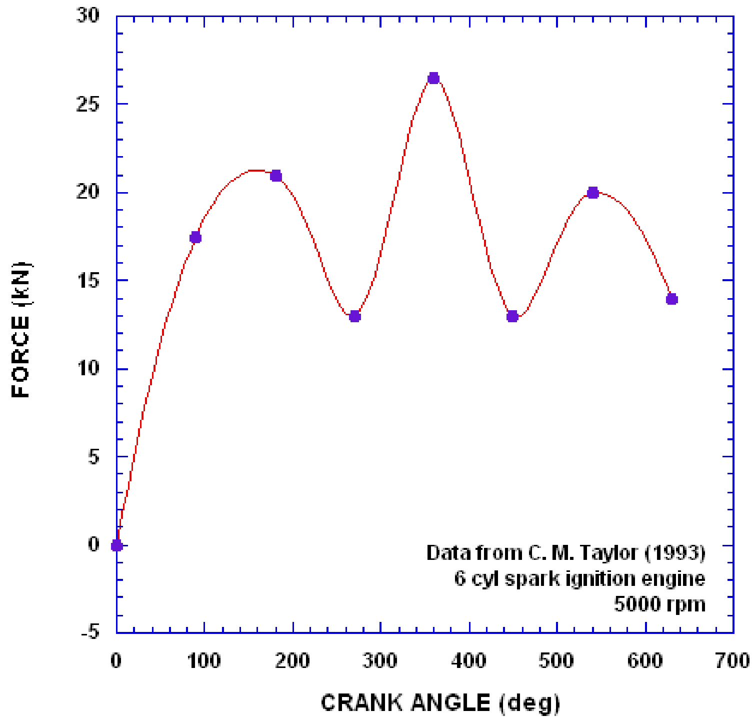

Figure 5. Bearing forces as a function of crank angle in a fired engine (based on data from [9]).

Research plan. This project was comprised of two phases. The first was a pre-screening and materials acquisition phase using existing friction and wear testing equipment, and the latter was intended as a better simulation of lubricated conditions. It used a specialized apparatus which was designed and built during the period of Phase 1.

Phase 1: *Surface Technology Review and Pre-Screening Experiments*. Following an in-depth literature review and discussions with industry contacts, over twenty surface treatments and coatings for Ti alloys were placed on a candidates list. Titanium alloys to be used as the substrate and a reference bearing material were obtained. ASTM standardized friction and wear tests (using ASTM G133, whose development was led by ORNL during the 1990s) were performed using engine-conditioned diesel drain oil. Also during Phase 1, a variable-loading ('spectrum loading')bearing materials test system (herein called the VLBT) was designed and built in order to provide the ability to simulate the variable contact and lubrication conditions experienced by connecting rod bearings in service. The ability to study such transient effects enabled more realistic screening of bearing performance than traditional friction and wear tests which operate under constant load and speed.

Phase 2: Simulative Testing in the Spectrum Loading Bearing Apparatus. The leading candidates for surface engineering Ti alloys, as determined from Phase 1, were tested in the VLBT under load spectrum conditions. A comparison could be made between friction and wear results from Phases 1and 2 to determine the extent to which the choice of screen test protocol affected material rankings. The salient results, summarized here, provide the basis for a series of recommendations on using Ti alloys for bearing surfaces in engine components like connecting rod big end bearings, cam lobes, and others.

4.2 Phase 1 Test Results

A standard reciprocating pin-on-flat test was selected for the Phase 1 screening of the surface treatments because it provides high contact stresses and allowed comparison with previous studies under the same conditions. Such severe test conditions focused more on material effects than lubricant properties, and thus provided a more conservative approach in selection of surface treatments and coatings.

Phase 1 screening tests, whose details are also described in two papers arising from this work [10-11], were conducted using ASTM standard G133 [12], a linearly-reciprocating ball-on-flat geometry. Test parameters are given in Table 4. Procedure A was used for baseline materials of Ti64 and bearing bronze (CDA 932), while Procedure B was used for all the tests in a modified form by using only 3-4 drops of the engine conditioned 15W40 oil at room temperature. The lubricant used in these tests was drain oil from a standard Mack T-11 test [13] and contained soot and acids.

Table 4. ASTM G133 Linearly Reciprocating Pin-on-Flat Test Conditions

Variable	Procedure A	Procedure B
Applied load (N)	25	200
Stroke length (mm)	10	10
Oscillating frequency (cyc/s)	5	10
Test duration (s)	1000	2000
Sliding distance (pin) (m)	100	400
Atmosphere	Air	Air
Humidity range (%RH)	40-60	Not specified
Method of lubrication	None	Immersion
Temperature of lubricant (C)	Not applicable	150*
Air temperature (C)	19 – 25	Not specified
Slider ball diameter (mm)	9.53	9.53

* For this work, the lubricant was used at room temperature. Therefore, results are reported as being performed under a modified Procedure B.

Tests were conducted using a 1989 vintage commercial reciprocating test apparatus (Plint model TE77, Phoenix Tribology, UK). AISI 52100 high Cr bearing steel was used as the standard counterface (ball) material, but a few experiments were also conducted using a silicon nitride ceramic (NBD 200, Norton-St Gobain Ceramics). Friction measurements were made using data acquisition software (LabView™) at 200 Hz, recorded and averaged for 1 second at 5 second intervals. Therefore, there were 2×10^5 friction coefficient data points collected for each Procedure-A test and 4×10^5 points for each Procedure B (mod.) test. The surfaces of the flat specimens (25 x 25 mm square) were polished with 400-grit, 600-grit and 1 µm diamond paste. Both the ball and flat specimens were cleaned in acetone and isopropanol prior to testing.

Wear volumes for the flat test coupons were measured using a vertical scanning interferometer (VSI) (Wyko ™ NT9100, Bruker Instruments) and processed using the accompanying software. Examples of images used for wear measurements are shown in Figures 6(a) and (b). The wear volume of the pin specimen (a fixed ball) was estimated by measuring the diameter of the wear scar on the tip under a microscope and then using the equations listed in ASTM G133.

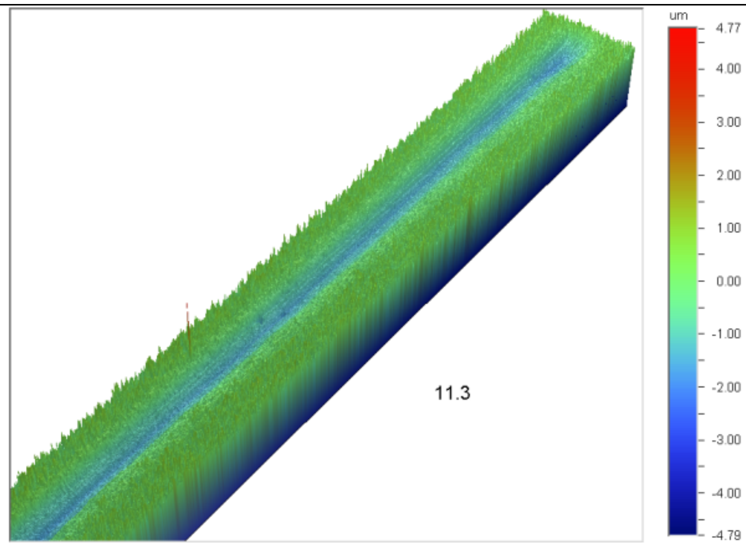

(a)

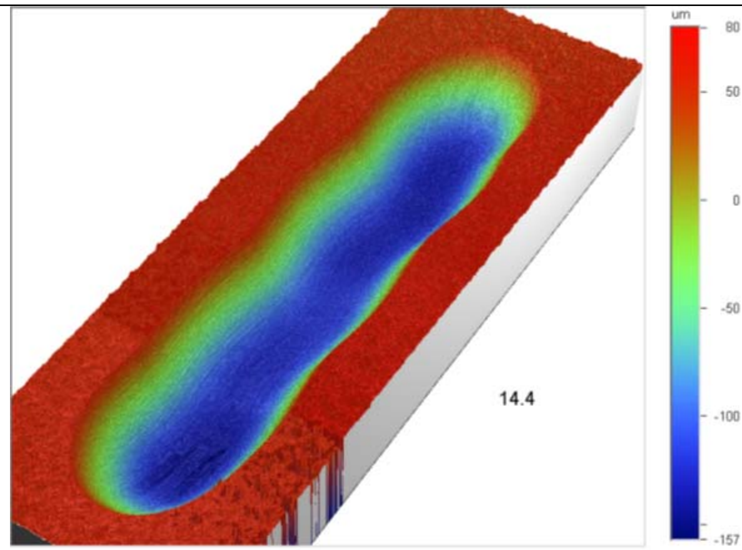

(b)

Figure 6. 3-D reconstructions of VSI images of wear tracks of (a) a completed test of OD Ti64, and (b) a prematurely terminated test of carburized and shot-peened Ti64 in which the wear was excessive.

Table 5 lists different materials and surface treatments investigated in Phase 1, along with corresponding Vickers and Knoop hardness (100 g-f load), the surface roughness parameters, and the identification codes of the test coupons used in Phase 1. Barring severe wear or premature test cessation, three tests were conducted for each candidate material/treatment. A description of each material, its treatment, and its source is provided in Appendix A. Indentation hardness values are the average of 8−12 indents per test coupon and the corresponding standard deviation is also listed. The arithmetic surface roughness (Ra) and root-mean square roughness (Rq) were measured at 6 − 8 locations on the flat test coupon surfaces using the same VSI that was used for wear measurements.

Table 5. Phase 1 Test Coupon Materials, Surface Finish, and Hardness

Category	Material or Treatment	Designation	Roughness R_a (μm)	Roughness R_q (μm)	HV (GPa)	HK (GPa)
Bulk materials	Ti-6Al-4V alloy	Ti64	0.067	0.087	3.64 ± 0.11	3.73 ± 0.11
	Bearing bronze	BB	0.032	0.05	1.1 ± 0.06	1.1 ± 0.06
	Nitinol (60Ni-40Ti)	60NiTi	0.011	0.015	3.81 ± 0.13	3.59 ± 0.15
Thermal and chemical treatments	Oxygen diffusion	OD	0.31	0.38	7.1 ± 0.76	8.59 ± 0.5
	Nitriding	NR	0.12	0.157	6.96 ± 0.26	7.37 ± 0.15
	Carburizing	CR	0.124	0.16	6.92 ± 0.31	7.03 ± 0.22
	Nitinol + heat treatment	60NiTi + HT	0.3	0.376	10.11 ± 0.73	15.55 ± 0.75
	Anodizing	TZ	0.633	0.811	**	6.93 ± 0.4
Coatings	Ti64 + TiB_2 microcomposite	IR	0.218	0.282	6.16 ± 0.27	5.45 ± 0.67
	Al-Mg-B nanocomposite	NAMB	0.054	0.075	*	7.1 ± 0.24
	Diamond like carbon coating	DLC	0.06	0.082	4.14 ± 0.46	4.56 ± 0.10
	TiN coating	TiN	0.118	0.153	7.1 ± 0.36	10.29 ± 0.47
	CrN coating	CrN	0.056	0.07	4.61 ± 0.11	7.1 ± 0.24
	Cu-Ni-In coating on BB	CuNiIn−BB	8.17	10.26	**	**
	Cu-Ni-In coating on Ti64	CuNiIn−Ti64	11.46	14.5	**	**
Mechanical treatments	Shot peening Ti64	SP	3.98	5.03	**	**
Duplex treatments	Oxygen diffusion + shot peening	OD + SP	2.57	3.23	**	**
	Nitriding + shot peening	NR + SP	2.14	2.69	**	**
	Carburizing + shot peening	CR + SP	2.09	2.65	**	**

Notes:
* Invalid data due to indentation fracture. There was a relatively soft substrate under a hard, thin coating
** Surface was too rough to measure the indent dimensions accurately

Pass-Fail Criteria for Lubricated Tests. 'Pass' criteria for lubricated ASTM G133 Proc. B(Mod) tests were based on a friction coefficient of less than 0.15, and a stable and non-vibratory behavior throughout the entire duration of the run. Some tests vibrated or squealed so badly, that a complete test could not be completed. Others that failed had severe wear damage or wore so quickly that the test had to be stopped to avoid damaging the specimen holders.

Non-lubricated wear of baseline couples. Table 6 lists the wear volumes of the flat coupons and the balls for non-lubricated baseline tests (ASTM G133, Proc. A). This geometry (a concentrated point load oscillating on a surface) typifies a worst case scenario because the contact stress is high and a stable lubricant film cannot form as the sliding speed rises and falls. From Table 6, the total wear volume for Ti64 against 52100 steel is about 30% greater than that of the baseline bronze alloy against the same ball material. This performance is unacceptable.

Table 6. Wear Volumes (V_w) from Non-lubricated Tests

Sliding pair (flat specimen / ball)	V_w, flat specimen (mm^3)	V_w, steel ball (mm^3)	Total wear (mm^3)
Ti64 / 52100 steel	1.16	0.008	1.171
CDA 932 BB / 52100 steel	0.897	0.0017	0.899

Lubricated friction and wear results for Task 1. Figure 7 summarizes the frictional data from the Task 1 screening tests using the conditions shown in the right-hand column of Table 4. In addition to a friction coefficient criterion of < 0.15, unstable sliding or excessive wear behavior further reduced the number of candidates selected for Phase 2.

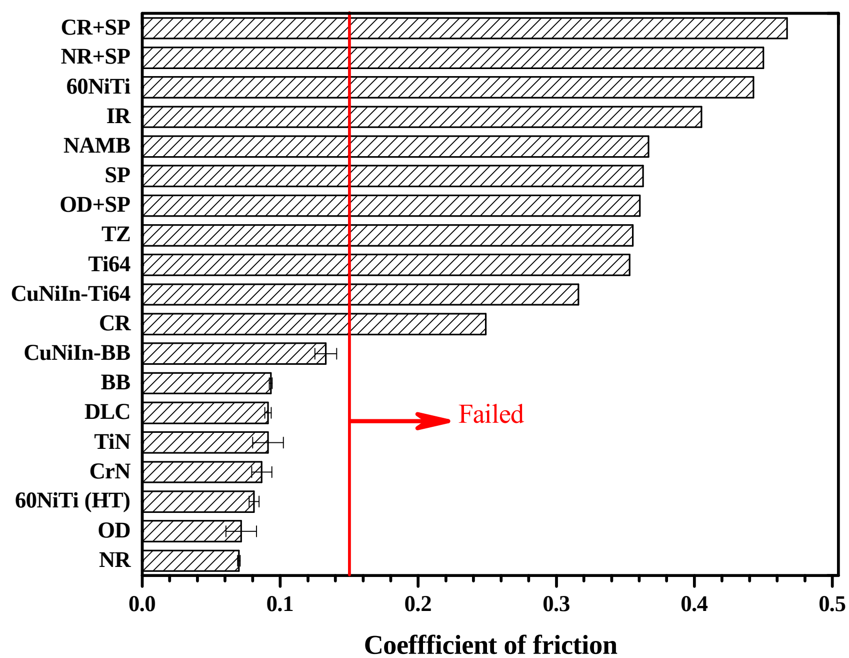

Figure 7. Average steady-state friction coefficients for candidate surface treatements under lubricated conditions, including data for the baseline bronze (BB) which passed, and the bare Ti64 which failed. Treatment code designations may be found in Section 9 and descriptions in Appendix B.

Figure 8 displays the three-test average wear volumes of both coupons and ball materials subjected to lubricated tests in which all three repeated tests ran to completion without the need for premature termination. The wear volumes of the coupons are presented on the right hand X-axis and the wear volume of the balls is plotted on the left hand X-axis. Note that the split axis uses different length scales on the left and on the right.

Of the coated specimens, CrN coated Ti64 showed the least amount of wear, followed by DLC coated coupons. Of the heat treated specimens, OD treated Ti64 coupons showed the least amount of wear. Tests with the Cu-Ni-In electro-coated BB (CuNiIn − BB) specimen produced the largest amount of wear on both the flat coupon and the balls, but the coating is soft and is intended as a sacrificial, running in coating. Among Ti alloys, the heat-treated 60NiTi custom-cast alloy (60NiTi + HT) shows the most wear on both the flat coupon and the ball. Since the wear volume of the coupons is orders of magnitude larger than the wear volume of ball specimens, the ranking of the treatments remains the same even when total wear volume of both the counterfaces is considered. Photomicrographs of wear specimens and cross-sections thereof may be found in Bansal et al. [10] and are not reproduced here.

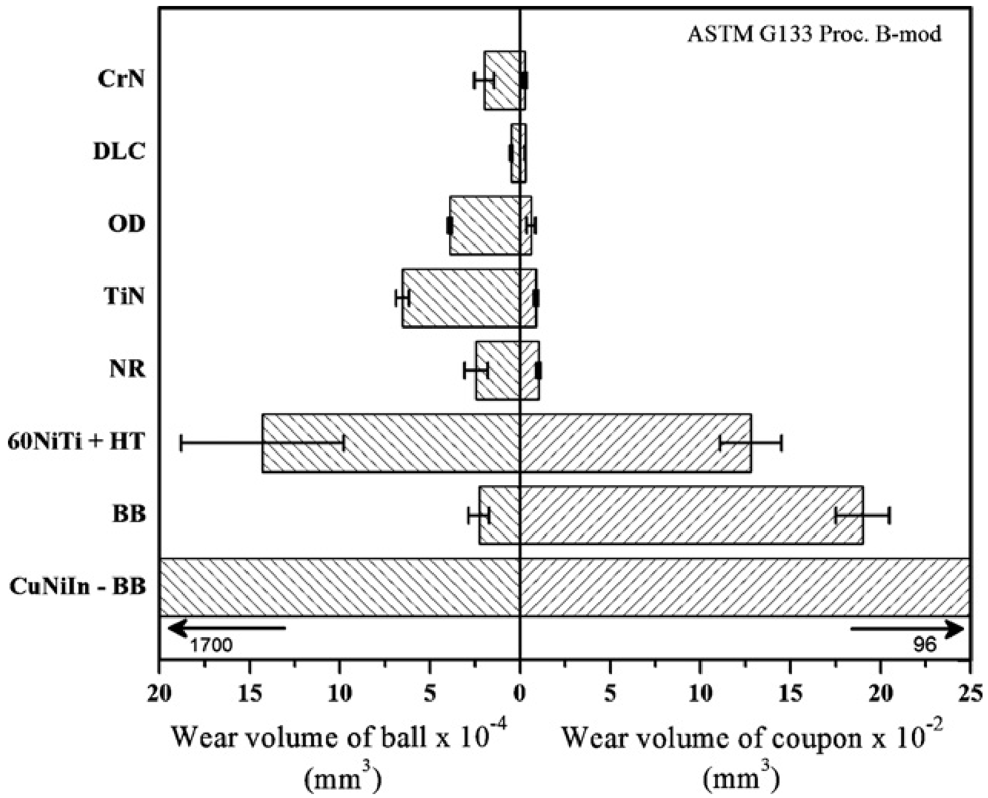

Figure 8. Comparison of the wear volumes of the ball (to the left of the center) and the flat coupon (to the right of the center) from [10].

Effects of Mechanical Working in addition to Diffusion Treatments. Additional studies on the tribological effects of surface treatments that combined mechanical working with diffusion treatments were performed early in 2012 [11]. Those experiments also used ASTM G133 (Procedure A) with parameters listed in Table 4. No lubricant was used in order to emphasize the material effects. Furthermore, two different slider materials were used: 440C stainless steel and silicon nitride (NBD 200, St. Gobain-Norton).

The diffusion treatments (done prior to mechanical treatment) were:

- Carburizing
- Nitriding
- Oxygen diffusion

The mechanical treatments applied to the coupons were:

- Shot peening
- Planishing

Shot peening of Ti64 is used extensively to improve its fatigue strength. It introduces residual compressive stresses into the surface. The shot peening in this work was done by a commercial facility (see Appendix A) using the following parameters: 230H cast shot with 0.008-0.012″ A (Almen intensity) and coverage of 125% . Planishing is a process of repetitive impact with a rounded hammer. It is typically used for decorating or forming sheet metal, or for repairing damage in sheet metal such as in auto repairs. In the current case, planishing used a rounded-end (ball peen) hammer weighing 586 g, and with radius of curvature of approximately 25 mm. Starting with a titanium coupon polished with 600 grit wet SiC paper, hundreds of impacts were made to work harden the surface. After planishing, the Rockwell hardness of the Ti64 surface had risen from HRC 37.7 to HRC 48.

Table 7 lists the arithmetic average surface roughness (Ra) and ten-point height (Rz) of the pre-test coupons in various treated conditions, including the bare Ti64 substrate. Since some of the surface treatments were only tens of micrometers deep, it was not felt to be practical to attempt to final-polish the specimens after applying the combined surface treatments, but rather to leave them as-is. This may have affected the wear-in characteristics of the coupons, but in most cases, the wear rate would have quickly worn through the initial roughness.

Table 7. Pre-Test Roughness of Bare and Treated Titanium Alloy Specimens
(Ra = arithmetic average roughness, Rz = ten point height, 6 measurements)

Treated Condition	**Ra (μm)** Average (std. dev.)	**Rz (μm)** Average (std. dev.)
Bare Ti64	0.213 (0.03)	2.07 (0.36)
Planished only (PL)	0.195 (0.02)	1.60 (0.35)
Shot peened only (SP)	2.953 (0.25)	15.87 (1.03)
Nitrided + shot-peened (NR + SP)	1.617 (0.08)	8.35 (0.51)
Oxygen diffused + shot-peened (OD + SP)	1.955 (0.24)	10.98 (1.60)

Subsurface Microstrain Characterization. In addition to surface finish measurements and hardness testing, the degree of surface damage imparted by the various treatments was investigated using X-ray diffraction (XRD) line broadening analysis. Diffraction peaks broaden due to crystallite size and microstrain [14]. Smaller crystallites cause broader peaks, but the effect is negligible for crystallite sizes greater than approximately 100 nm. Microstrain includes any effect causing a non-uniform, local variation in lattice spacing, such as composition gradients and stacking faults. For a ductile metal such as Ti, the largest source of microstrain broadening is dislocations. Size and strain broadening effects may be distinguished by their dependence on the diffraction angle. The peak areas remain constant, and therefore peak broadening is accompanied by a reduction in peak height.

Diffraction patterns were collected with a PANalytical X'Pert Pro diffractometer in Bragg-Brentano geometry with Cu Kα radiation (λ=1.5406 Å). With Cu radiation, the penetration depth (99%) into Ti64 is estimated to be 5-16 μm, depending on incident angle. Because the typical depth of the surface-affected zone was on the order of 100 μm, the measurements were restricted to the affected zone. The data were fit using the LeBail method with the pseudo-Voigt profile function and using the Cagliotti equation to fit the peak widths. The microstrain (ε) may be determined from the peak widths as in the following equation $\varepsilon = B_{strain}/(4\tan\theta)$, where θ is half the diffraction angle and B_{strain} is the peak broadening due to strain obtained by removing the instrumental and size broadening from the total measured peak widths [14].

A silicon standard was used to remove the instrumental effect from the total broadening. Preliminary analysis indicated negligible size broadening, and therefore it was assumed to be zero. Additionally, the microstrain was assumed to be isotropic. A more in-depth analysis could account for anisotropic broadening arising from preferential slip directions [15], but is beyond the scope of this work. The microstrain was calculated from the peaks of α-titanium, which was the major phase in all samples. Traces of β-titanium were observed in the non-treated and planished samples, and traces of nitrides (namely Ti_2N and TiN) were observed in the nitrided samples.

The microstrain values are shown in Figure 9. The Ti64 sample without any additional surface treatment beyond the as-received condition has the lowest value, as expected. Of the two mechanical surface treatments, shot peening resulted in a much higher level of microstrain than planishing. Diffusion treatments with oxygen and nitrogen alone contribute to the measured microstrain, likely due to chemical inhomogeneity in the metal and/or the metal-oxide/nitride interface stresses. The combination of diffusion treatment with shot peening gave similar results to shot peening alone. The increase in microstrain arising from diffusion treatment may be offset by a reduction in microstrain arising from dislocations, due to shielding of the underlying metal due to the surface oxide or nitride.

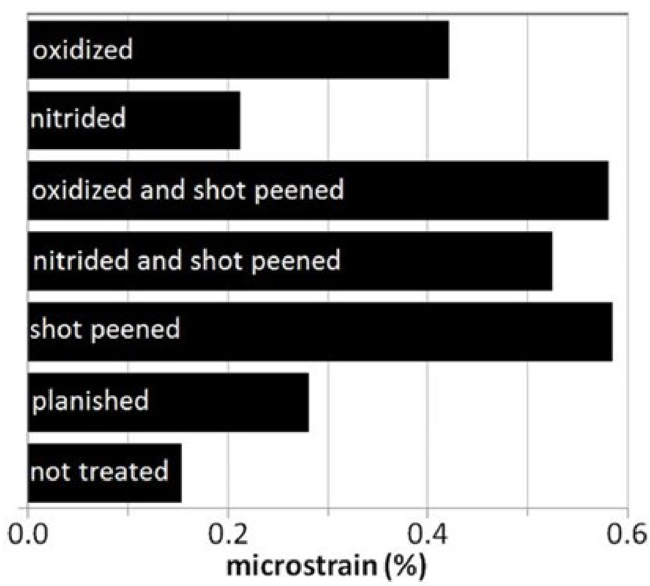

Figure 9. Comparison of subsurface microstrains for various treatments of Ti64.

Friction and Wear Results. The most pronounced effects of combined treatments were observed in the frictional behavior, as exemplified by Figure 10. Without treatment, the kinetic friction coefficient of the materials couple rose quickly to about 0.4-0.5. With the combined surface treatment, there was a delay, and a lower friction initial period preceded the transition. The choice of ball material also seemed to affect the duration of the lower friction period, with the 440C ball delaying the transition to higher friction by about 3 meters in sliding distance relative to the ceramic ball.

Since friction force times distance equals frictional work, the longer a sliding couple remains at low friction, the less energy is available to do work on the materials – i.e., to produce wear. Therefore, one would expect less total wear for the tests in which there was a lower friction period. The data in Table 8 show that this effect was relatively minimal. In all but one case (NR+SP), the low friction period was less than 10% of the total sliding distance. In the case of (NR+SP) coupons rubbed on 440C steel was there a discernible effect of the low friction period on reduced wear volume.

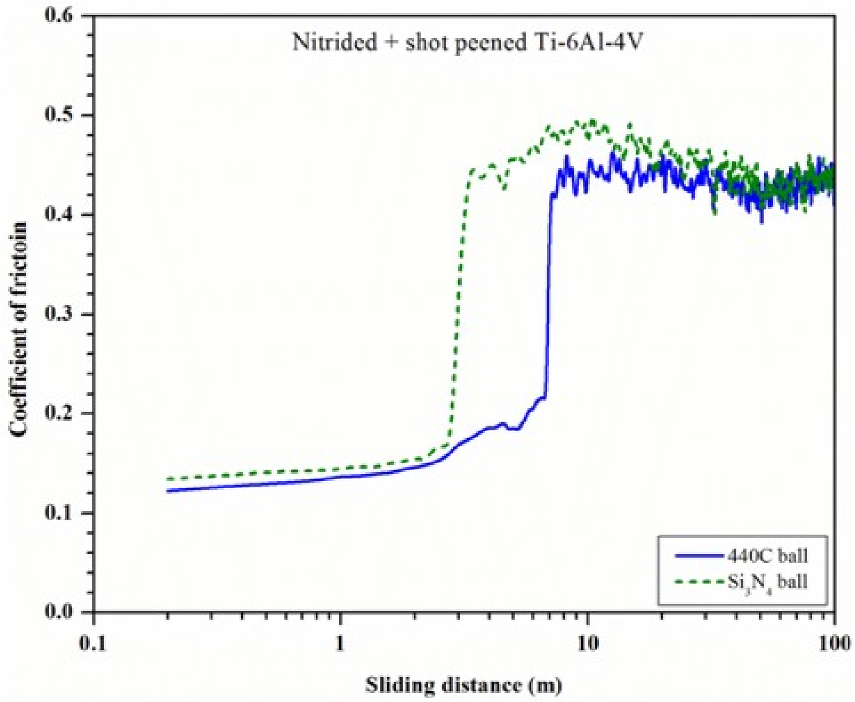

Figure 10. Friction transitions during initial period of sliding of NR+SP coupons against two ball materials. In both cases the initial and final friction coefficients were about the same.

Table 8. Friction Transition Distances and Wear Volumes of Surface Treated Ti64 Coupons

Slider material	Treatment	Test	Sliding distance to friction transition (m)	Wear volume, flat specimen (mm^3)
440C st steel	PL	1	none	0.986
		2	none	1.121
	SP	1	none	0.985
		2	none	1.103
	OD + SP	1	6.8	0.901
		2	4.6	1.012
	NR + SP	1	8.1	0.802
		2	23.2	0.823
Silicon nitride	PL	1	none	1.124
		2	none	1.025
	SP	1	none	1.185
		2	none	1.143
	OD + SP	1	0.4	1.066
		2	0.8	1.050
	NR + SP	1	2.6	1.062
		2	1.2	1.097

The primary conclusions and observations of studies of combined treatments are:

- The choice of a counterface material, whether 440C stainless steel or bearing-grade silicon nitride, had little effect on long-term friction trends. However, for combined diffusion treatments plus mechanical working, the 440C balls displayed longer initial low friction period before transitioning to the higher friction typical of non-treated Ti alloy.
- The choice of counterface material had no evident effect on the wear of shot peened or planished (mechanically-worked) Ti64 surfaces.
- Silicon nitride balls displayed transferred material from Ti64 from the flat coupons, but there was no significant difference in the wear amount from one treatment to another.
- The combination of nitriding with shot peening yielded the lowest wear results when sliding against 440C.
- Planishing and shot peening added to the near-surface microstrains in the non-treated Ti64 specimen.
- Oxygen diffusion and nitriding treatments increase the microstrain, but did not raise the microstrain levels as high as those from mechanical working alone.
- No obvious gradients in hardness were recorded beneath the wear track surface for sliding against either of the counterface materials, silicon nitride or 440C balls although there were some indications of a mechanically deformed layer.

In general, the sliding wear process for titanium alloy surfaces is so problematic that shallow diffusion treatments have little effect other than to prolong the transition to severe wear under non-lubricated sliding conditions. Additional details of this study, including microscopy, may be found in Ref. [11].

4.3 Development of the Variable-Load Bearing Test (VLBT) Apparatus

A programmable, variable loading, rotating cylinder-on-flat apparatus was designed and built to study the friction and wear of several non-ferrous alloys and surface treatments under variable loading conditions. The basic configuration of the VLBT is shown in Figure 11. A close-up is shown in Figure 12. The load is applied by a displacement-controlled, stiff ball screw that compresses a calibrated spring at the end of a primary load arm. A computer program varies the actuator movement according to a preprogrammed load spectrum, and hence the applied load on the stationary specimen that is pressed against a rotating cylinder of alloy steel. The load spectrum was based on a polar plot of the forces on a big-end bearing in an automobile engine that was published by Taylor [9]. The variations in the load with degrees of crank shaft rotation were scaled to fit the load range of 20-100 N that can be applied by the VLBT. To study frictional effects on the bearing surfaces at each load in more detail, the period of a single cycle was stretched to 120 s, whereas the whole sequence of load changes might take place in a fraction of a second in an actual engine operating at 1000-4000 rpm. The standard 120-second load profile for the majority of tests presented was comprised of the following sequence of forces and times: 36 N (10 s), 60 N (10 s), 80 N (10 s), 50 N (15 s), 75 (10 s), 100 N (10 s), 50 N (10 s), 75 N (10 s), 50 N (15 s), 80 N (10 s), 60 N (10 s), 36 N (10 s). This profile was repeated for a total of ten times. An example of the first two loading cycles is shown in Figure 13 for a test on a bearing bronze specimen against steel.

The surface speed used for the current experiments was 0.50 m/s. A peristaltic pump (showed at the rear of the view in Figure 10) dispensed one droplet of 15W40 diesel oil (Valvoline Blue™ diesel oil) about every 14 seconds, resulting in a delivery rate of 11.8 ml/hr, or about 3.93 ml for a 20 minute test. Friction force, normal force, and motor speed were sampled at a rate of 1000/s and the friction coefficient, averaged over 2 second intervals, was used to establish trends. The friction coefficient-load behavior during the last full test cycle was used to determine the post-running-in behavior for the various materials.

Typical wear scars on a bronze test specimen (CDA 932) against 8620 steel are shown in Figure 14. More testing details are provided in sections 4.3 and 4.4 of this report.

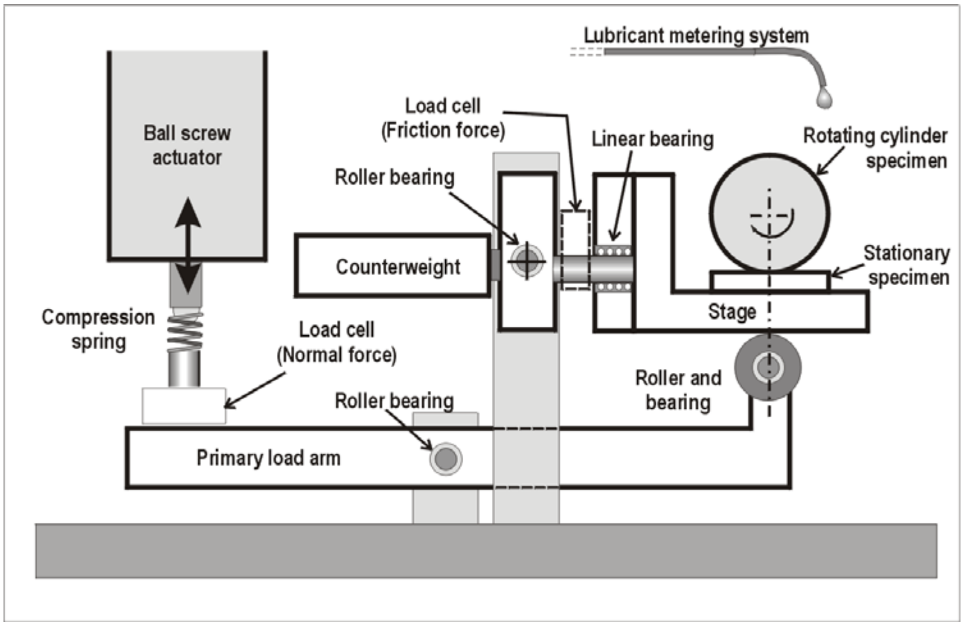

Figure 11. Schematic arrangement of the variable load bearing tester (VLBT).

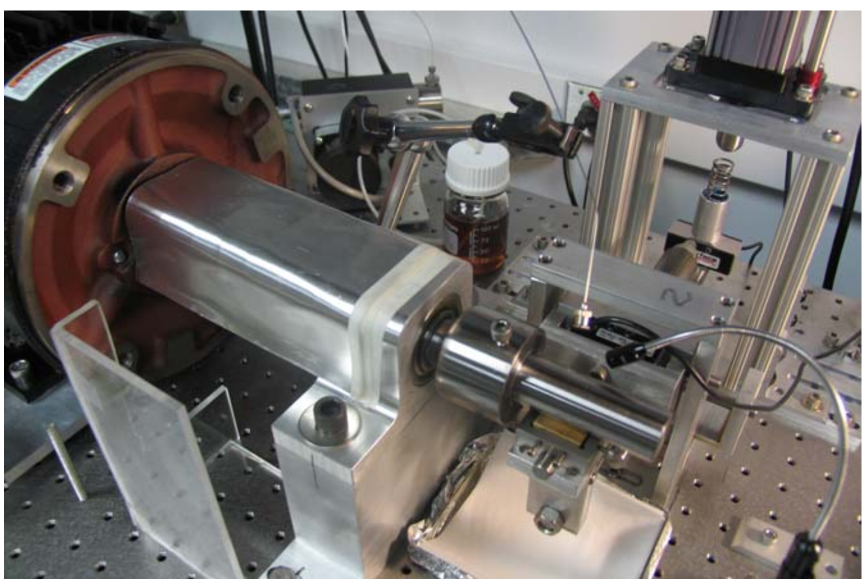

Figure 12. Close-up of the VLBT showing the rod specimen (lower right), the flat specimen pressed up underneath the rod, the stainless steel lubricant delivery tube (above the contact area), the load actuator (upper right), the oil pump (upper left, at rear) and the motor drive train (left).

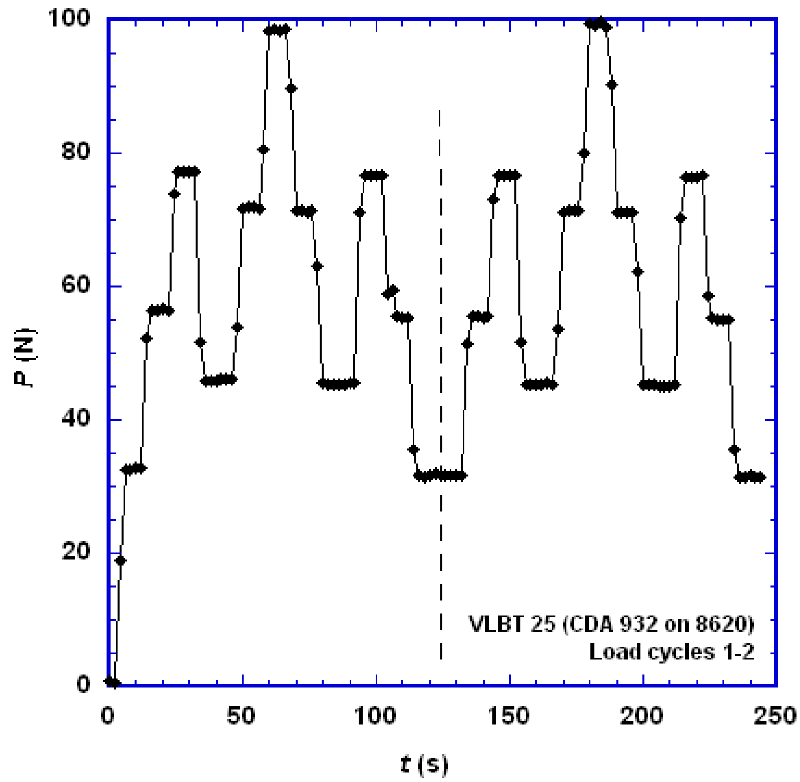

Figure 13. Load versus time for the first two cycles of a standard VLBT test.

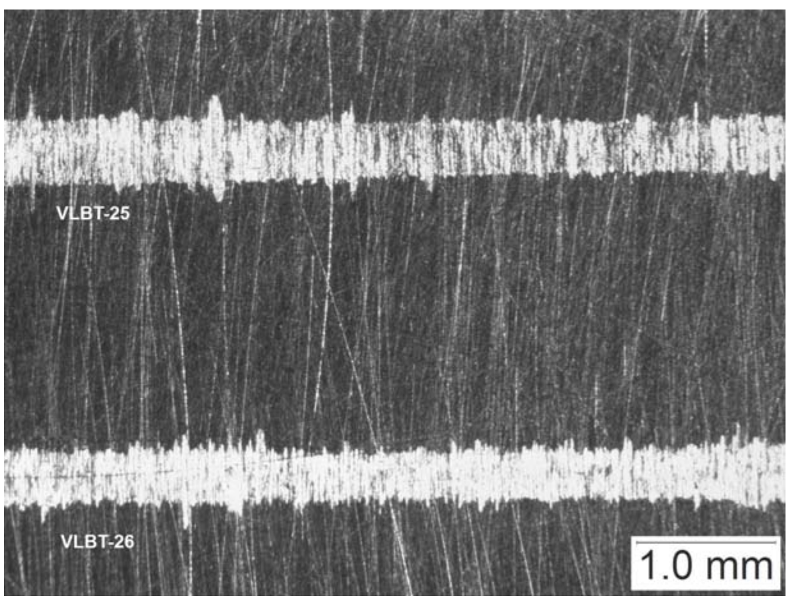

Figure 14. Two typical wear scars on a flat specimen (bronze) against alloy steel, produced on the VLBT. It was run for ten variable loading cycles lubricated with diesel engine oil.

4.4 Phase 2 Test Results

These results are also described in the proceedings of the 19th International Conference on Wear of Materials, to be published in *Wear* journal [16].

4.4.1 *Wear comparison between constant and variable load tests*. In early experiments with the VLBT system using Ti-6Al-4V on 8620 steel, a variable loading test having equal sliding distance and speed as constant load test (the constant load was the average of the variable loads) were compared. Figure 15 contrasts the friction coefficient behavior.

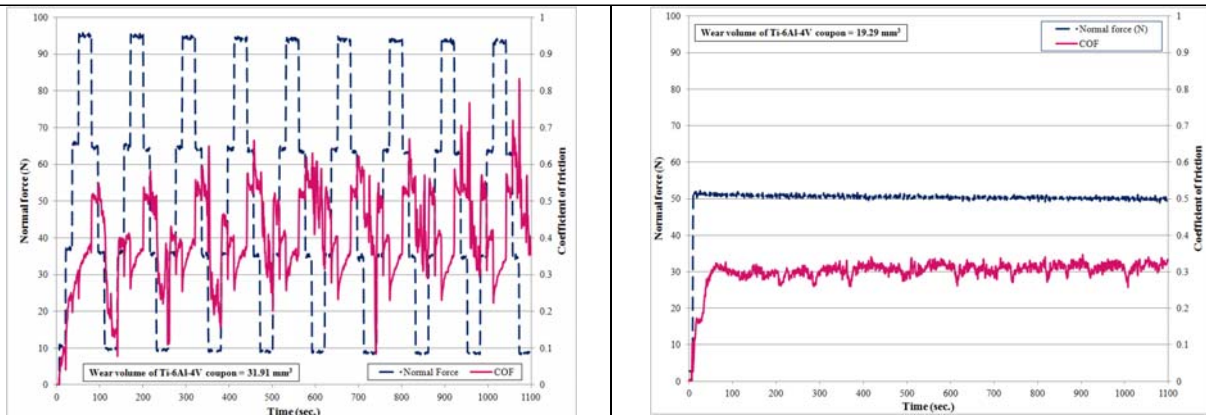

(a)	(b)

Figure 15. Comparison of load profiles and friction coefficients for a variable load test (a) and constant load test (b). In (a) the load is represented by dashed line and the friction coefficient solid lines. In (b) the friction coefficient is the lower of the two curves. The sliding speed, duration, and average normal force was the same for both tests. (Vertical scales are the same on both figures.)

As shown in Table 9, the wear volume of the flat specimen after testing was considerably larger for the variable load test than for the constant load test. This has significant implications for laboratory simulation of engine components because it is not sufficient to simply choose a nominal operating load for screening materials and lubricants. The load should vary similarly to the operating conditions.

Table 9. Comparison of Wear Volumes for Diesel Oil Lubricated Tests of 8620 Steel Against Ti-6Al-4V

	Wear volume of flat coupon, $V_{W,f}$ (mm^3)
Variable load test	31.91
Constant load test	19.29

4.4.2 *Running-in response*. In determining the length of standard tests for this work, it was desirable to ensure that the surfaces were sufficiently worn-in so as the data obtained would be representative of steady-state operating conditions. During the first few experiments, it was clear from the friction record that all test combinations would quickly run in to a steady state condition within less than one complete loading cycle. For example, the bronze ran in distinctively during the first ½ loading cycle (as shown in Fig. 16). After the initial steep friction transient, the friction coefficient versus normal force at steady-state was relatively stable (Fig. 17). By the 10th cycle, the friction coefficient for the bronze was quite stable, despite the changing loads (Fig. 18). As a result of initial experiments like these, the tenth cycle of spectrum testing was used as the standard to evaluate the friction coefficient versus load behavior of the candidate surface treatments and coatings.

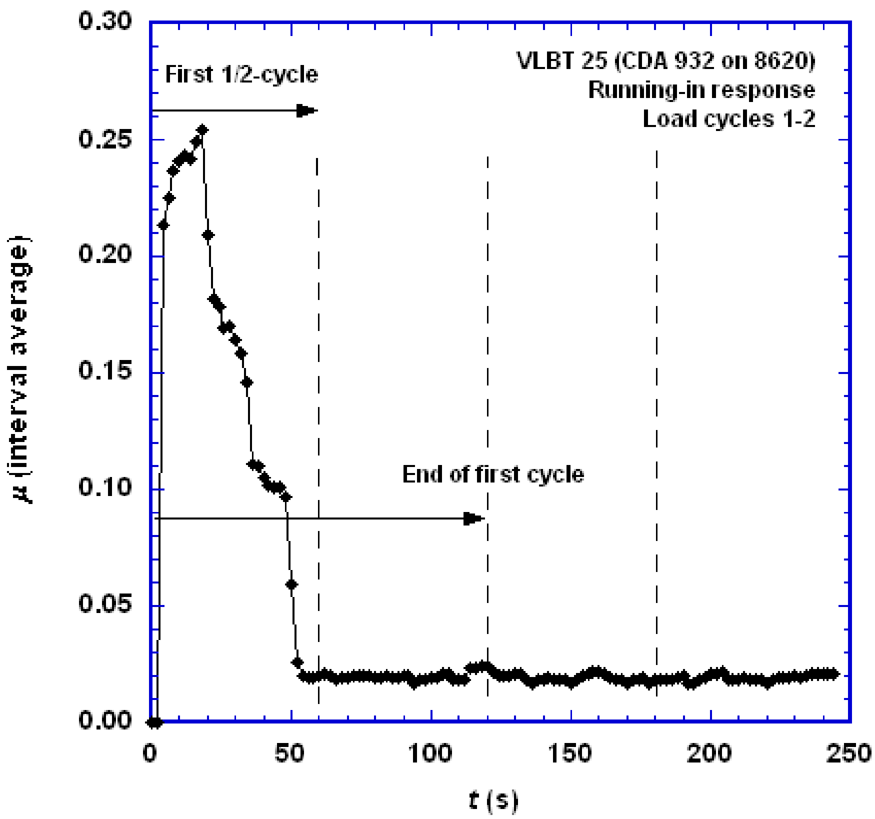

Figure 16. Running-in of bronze on 8620 steel during the first half cycle of the load spectrum.

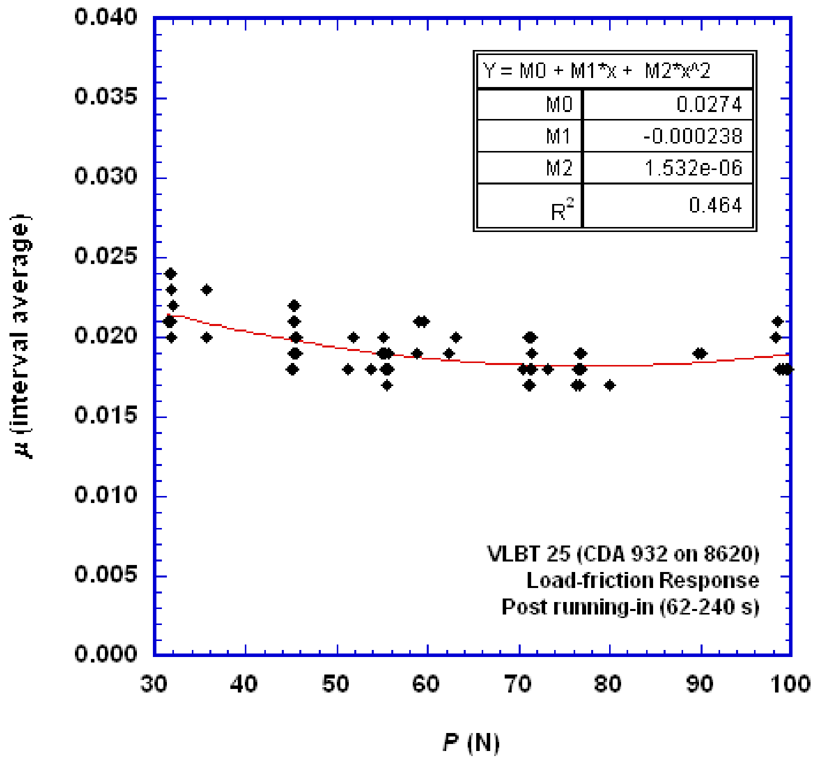

Figure 17. Post running-in friction versus normal force for the same run as shown in Fig 14.

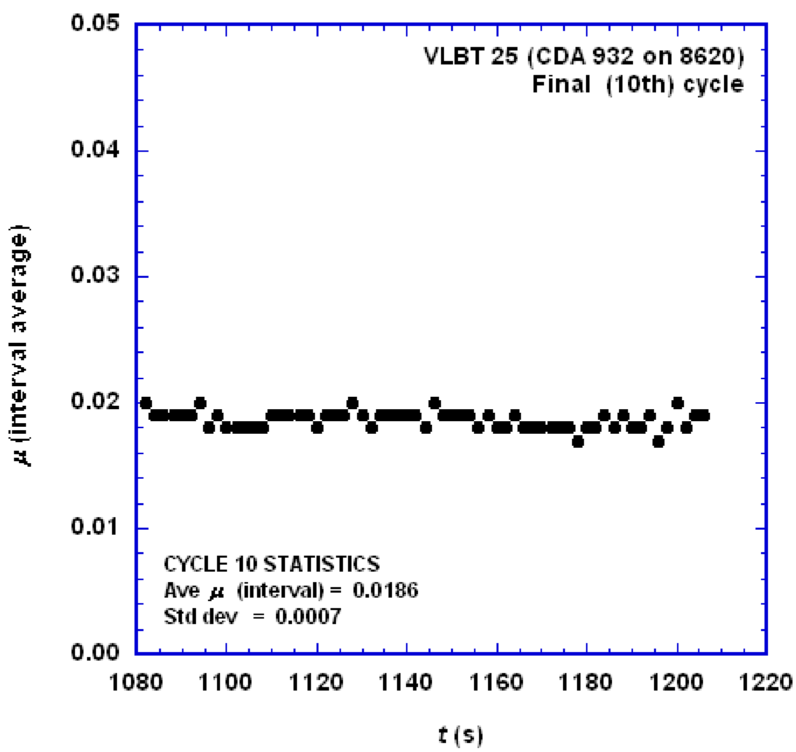

Figure 18. Friction coefficient versus time during the tenth cycle of spectrum loading of bronze on steel in diesel oil.

The film thickness/roughness ratio (Λ, see Fig. 4) is a useful descriptor of the lubrication regime. The numerator (*h*) is the lubricant film thickness in the bearing, which is usually calculated from lubrication theory [15] rather than measured. The denominator of that parameter is related to the root-mean-square roughness (σ_o) of the two opposing surfaces, thus:

$$\sigma_o = \sqrt{\sigma_1^2 + \sigma_2^2} \qquad (1)$$

During running-in (wear-in), the roughness of the softer of the mating surfaces tends to change more than the harder surface. If the process is one of asperity truncation, then the surface becomes smoother during wear-in. More often, both surfaces change somewhat during wear-in. However, if the load is high enough, the wear becomes more severe than simply truncating the sharper peaks on initial the surface finish and the post wear-in roughness increases.

Λ is affected by the wear-in of opposing surfaces, and friction coefficient tends to reach a minimum when $\Lambda \geq 3.0$. Considering that a high lambda implies a relatively thick lubricant film and separation of solid surfaces, then the effects of roughening or smoothing during wear-in can be demonstrated for several example cases, which start with both surfaces having σ = 0.5μm.

The effects of changing either σ_1 or σ_2 or both are plotted in Figure 19, assuming a constant film thickness of 1.0 μm.*

Case 1: σ_1 decreases (wears smoother) to 0.01 μm while σ_2 does not change

Case 2: σ_1 and σ_2 both decrease (wear smoother) to 0.01 μm

Case 3: σ_1 roughens up to 2.0 σ m while σ_2 does not change

Case 4: σ_1 and σ_2 both roughen up to 2.0 μm

It is presumed that some running-in occurs on every VLBT run; therefore, it would be presumptuous to use the initial surface roughness to estimate Λ at post run-in steady-state conditions.

---

* Measurement of actual film thicknesses in connecting rod bearings during engine operation is very difficult, so these values are usually calculated using one of several available theories. For example, Sun et al. [17] have calculated film thicknesses in internal combustion engine main bearings as a function of crank angle. The plot is shaped similarly to the triple-peaked behavior in Figure 11, except that the central peak is suppressed because the pressure in the film rises during the central spike, compressing the film. Values for the minimum lubricant film thickness range between 1.2 and 2.2 μm from the calculations reported in [17]. Other work on connecting rod bearings by Ross and Slaymaker [18] reports minimum film thicknesses, during 720 degrees of crankshaft rotation, ranging between 1.1 and 8 μm for a spark ignition engine running at 5250 rpm. Assuming 1.0 μm for *h* in Figure 17 seems reasonable for the purposes of illustration.

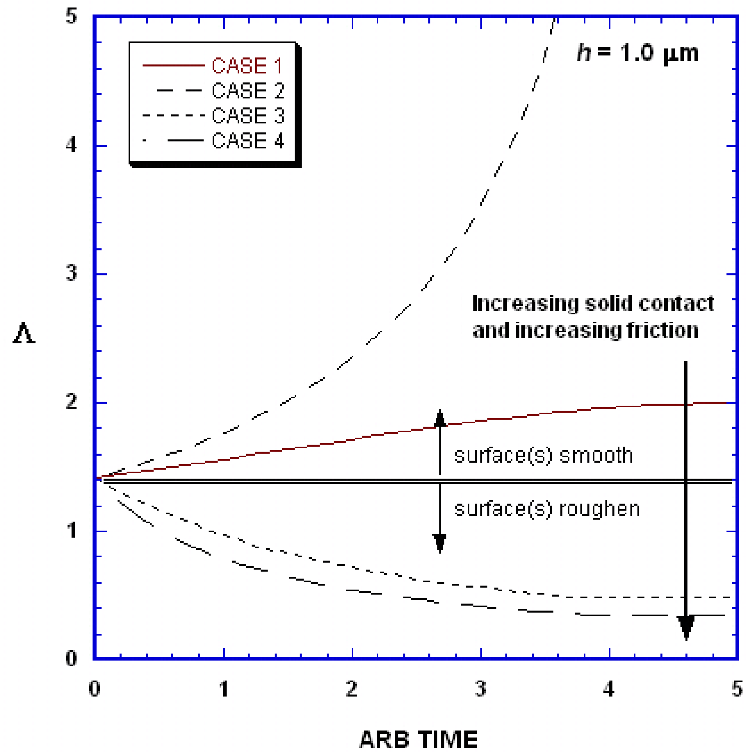

Figure 19. Effects of roughness on film thickness ratio as time passes (arbitrary time scale), given h = 1.0 µm.

4.4.3 Summary of friction data for various surface treatments. From the standpoint of lubrication regimes, VLBT operating point in essence moves up and down the Stribeck curve (e.g., Fig. 4) as the applied load cycles through its programmed variations (as indicated in Fig. 13). To examine that relationship friction coefficient data for the tenth cycle of each test were plotted not as a function of time, but rather versus the inverse load (P^{-1}) during the final cycle of the run. In each case, two experiments are plotted in the same figure to account for the repeatability of the data. In examining the plots in Figures 20-28**,** one is struck by the similarity of these plots to the bottom portion of Figure 4 which is the beginning of full film conditions in which friction tends reach its minimum.

Third-degree polynominal curve fits were applied to all the data presented in Figures 20-28 (see Appendix B for raw data). Two representative values, the friction coefficients corresponding to 30 N and at 100 N were calculated from those curve fits. Those results are summarized in Figure 29 to illustrate the maximum, minimum, and range of friction coefficient values obtained under steady-state lubricated sliding conditions. The reference material (Brnz) had the smallest range but the carburized surface, the CrN coated surface, and the HVPC coated surface all had lower friction levels during that cycle.

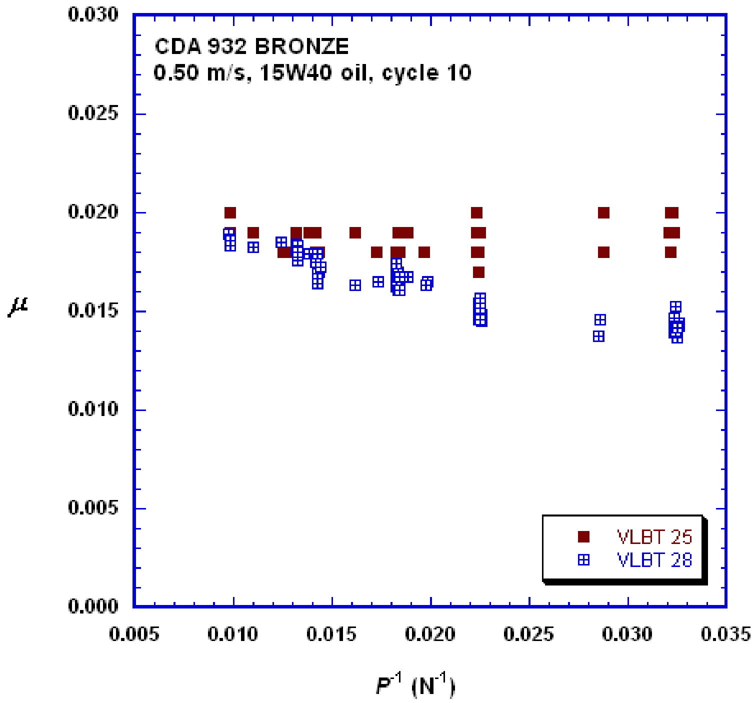

Figure 20. Friction coefficient versus inverse load for bronze.

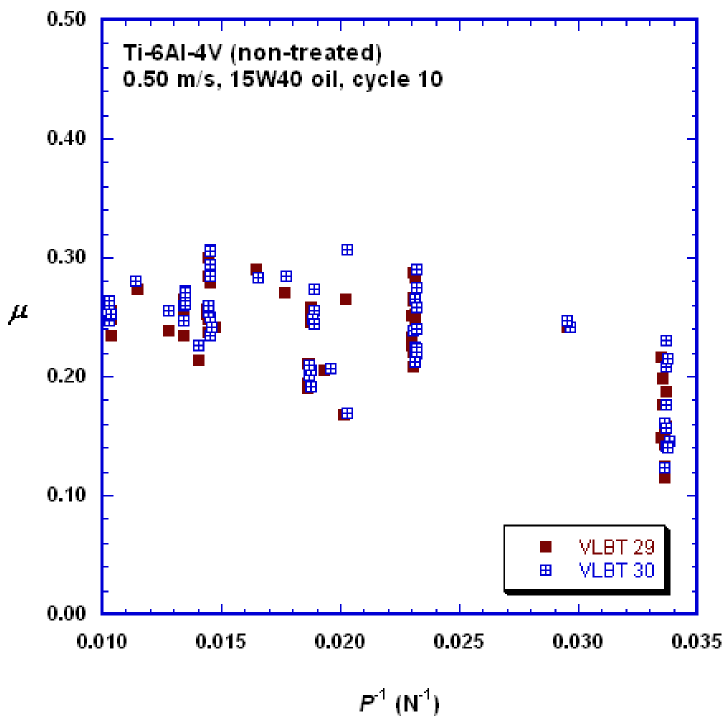

Figure 21. Friction coefficient versus inverse load for Ti64. Friction levels are associated with the boundary lubrication regime, and hence a different shaped curve than other combinations.

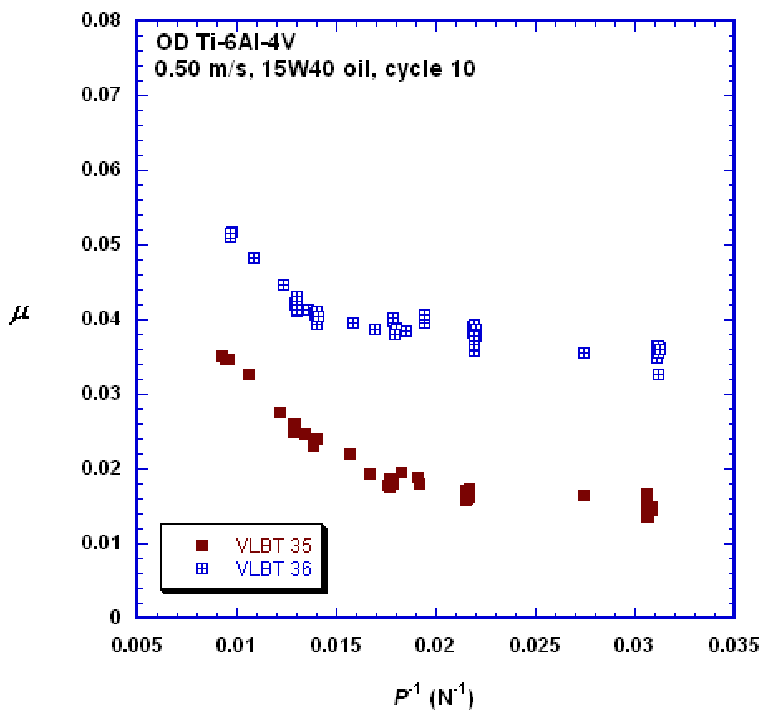

Figure 22. Friction coefficient versus inverse load for OD Ti64. The reason for the off-set curves is not known, because tests run both before and afterward suggest that the response was real and not a calibration artifact of some kind.

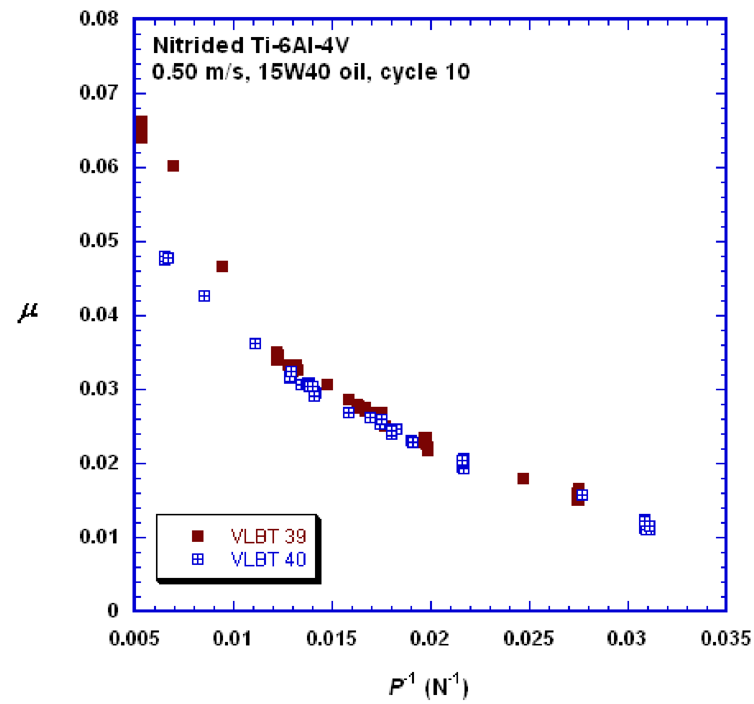

Figure 23. Friction coefficient versus inverse load for nitrided Ti64. Results at loads below 100 N (that is, $P^{-1} > 0.01$) were very repeatable. High load data tended to differ between runs.

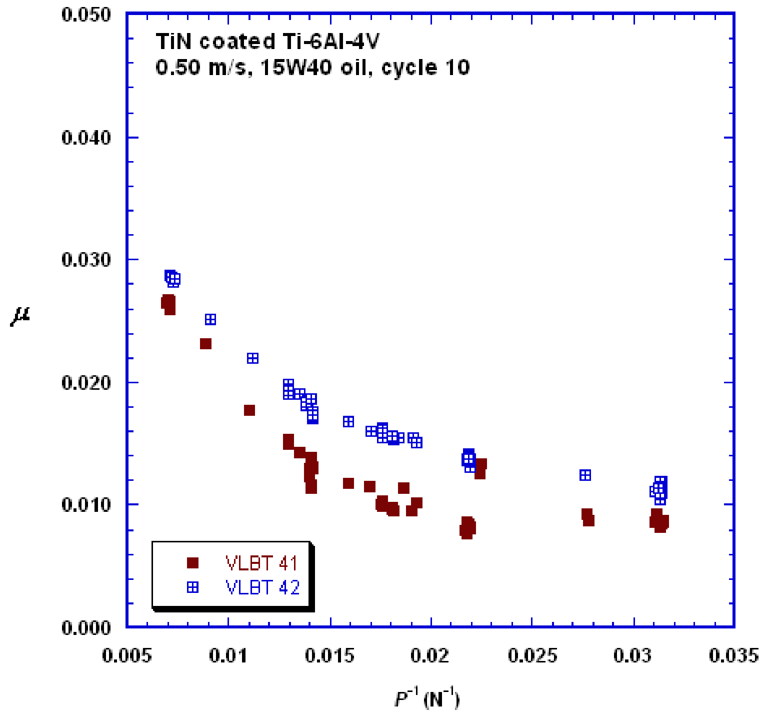

Figure 24. Friction coefficient versus inverse load for TiN coated Ti64.

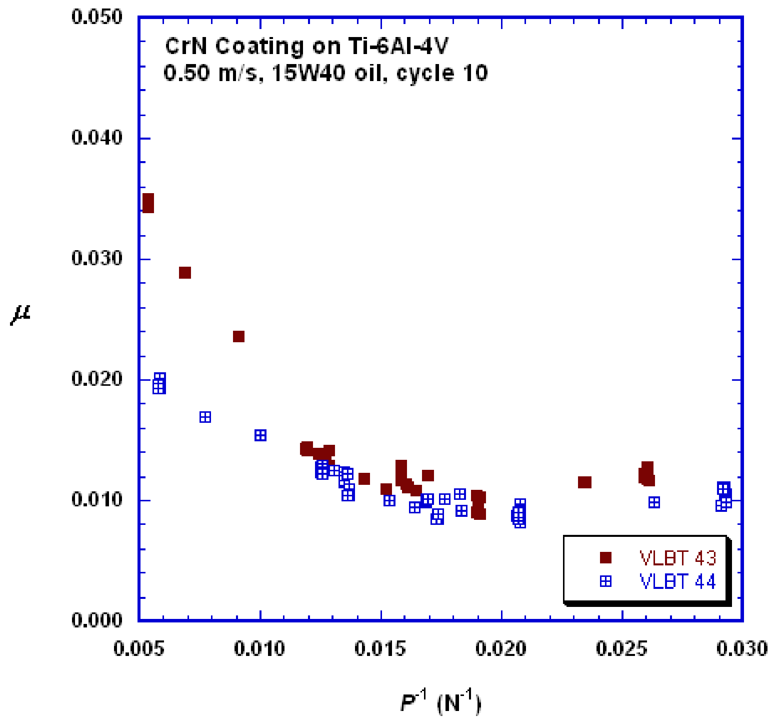

Figure 25. Friction coefficient versus inverse load for CrN coated Ti64

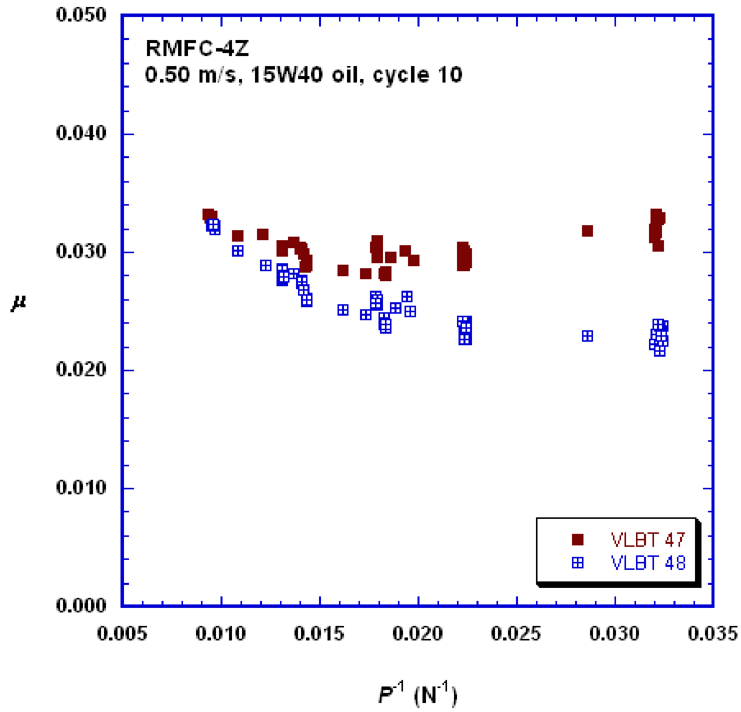

Figure 26. Friction coefficient versus inverse load for the polymer-filled anodic treatment (TZ).

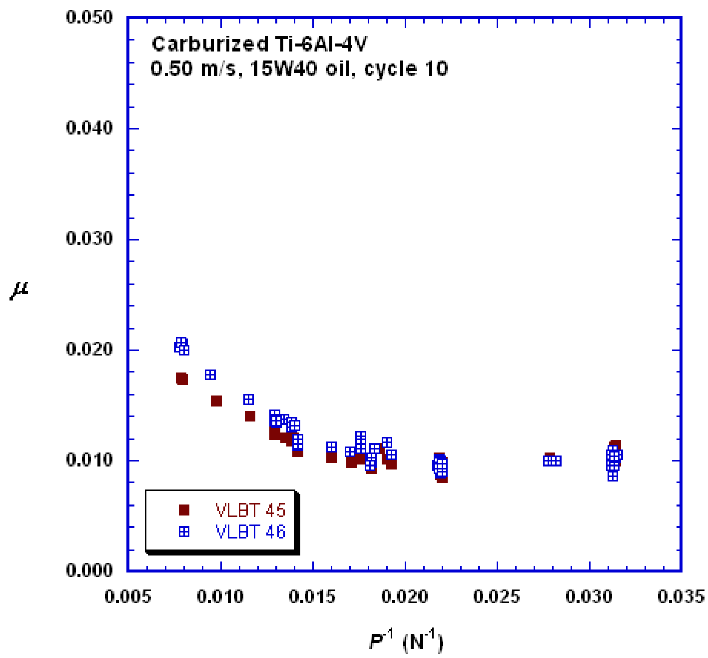

Figure 27. Friction coefficient versus inverse load for carburized Ti6. Friction coefficients were among the lowest of those measured in these experiments.

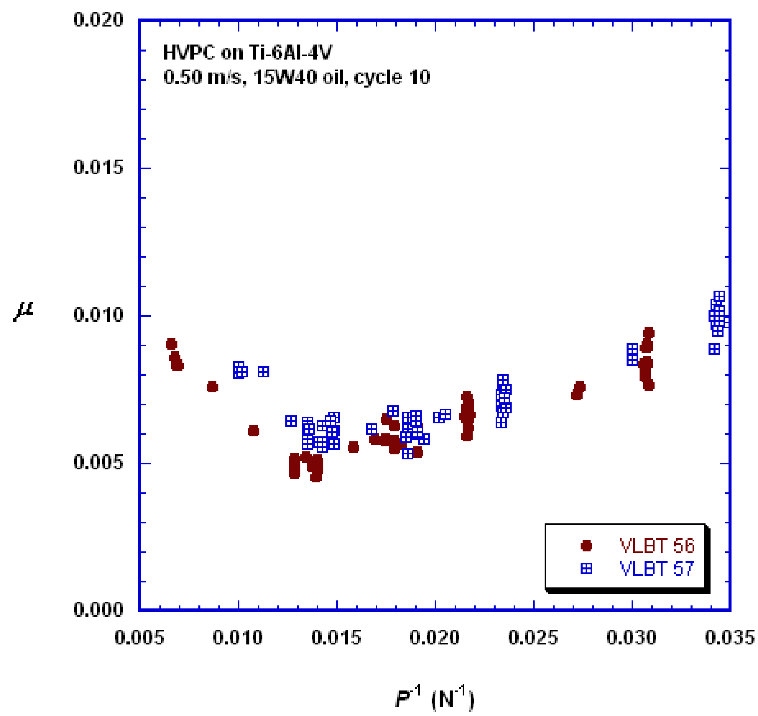

Figure 28. Friction coefficient versus inverse load for the high velocity powder consolidated coating from Pennsylvania State University.

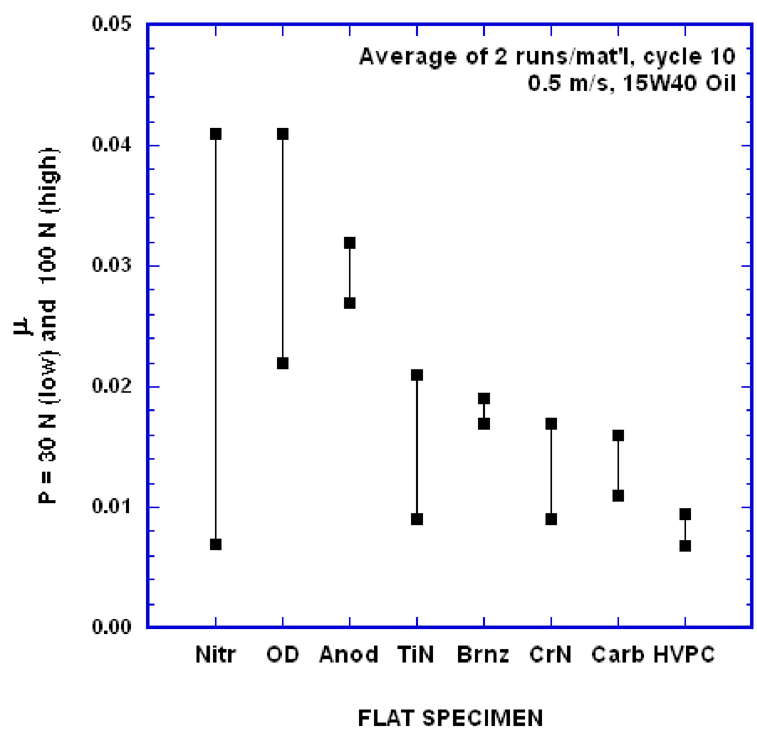

Figure 29. Summary of cycle 10 friction data showing the maximum, minimum, and range of friction. The reference material (Brnz) had the smallest range but three surface treatments had lower friction during the cycle.

4.4.4 *Wear surface examination*. Operating so closely to the mixed- and thick-film regimes produces little measurable wear damage and it is impractical to calculate an accurate wear rates for any of the test specimens except the most grossly worn Ti64 which is not of practical interest. However, microscope examination of the contacting surfaces distinguished some differences between the various surface treatments studied in Phase 2. Since the friction coefficients were not equal for the various material combinations, we must assume that the tribological behavior was not controlled by lubricant properties alone. In fact, the presence of surface features, to be described subsequently, indicates that the materials do play a role and that they do experience different degrees of wear despite a nominally mixed-film regime.

General Observations. General observations of the wear and surface contact features on the flat VLBT specimens are summarized in Table 10. Since the tests were mainly operating in a lubrication regime that allowed only rare solid-solid contact, it was not possible to quantitatively measure the wear volumes or estimate a wear rate. This practical consideration makes the prediction of wear lives for well-lubricated systems extremely difficult.

Table 10. Wear Features on Flat Specimens

Treatment	Test no. VLBT-	Observations of wear
Bare CDA 932	25,26	Even abrasion across the length of the contact zone.
Bare Ti64	29,30	Deeply scored wear scars with significant plowing and abrasion, suggestive of severe metallic wear. Friction levels consistent with boundary lubrication or starved boundary lubrication.
OD	35, 36	Pebbled reddish surface with numerous plateaus of bright, polished material and pitting indications as well. Suggests non-uniform wear and the potential production of hard particles removed by a mechanical pitting process. No abrasion indications like those on the bronze.
Nitrided	39, 40	Light wear scar with a few localized zones that displayed sharp scratches. Suggestive that the wear was generally mild except where an occasional debris particle could detach and run through the contact producing a scratch.
Carburized	45, 46	Faint, barely visible scar that did not run completely across the flat specimen, a few scuffed looking patches, and a few areas where some sharp scratches ran across the scar. Fewer scratches than for the nitride specimen.
TiN coated	41, 42	Very difficult to see any trace of wear, by eye or in the microscope.
CrN coated	43, 44	Very difficult to see any trace of wear, by eye or in the microscope.
Anod/coated	47, 48	There was a ground appearance to the unworn surface, running transverse to the sliding direction. Light polishing occurred in certain areas and the fibrous microstructure of the composite was revealed in those areas. A few more prominent scratches seem to run across the composite in the wear scar area and seemed to scratch continuously through the composite material all the way from the inlet side to the outlet edge of the scar.
DLC coating	(note 1)	Wore through to the Ti64 substrate, leaving jagged edges on the wear scar.

Note 1. Initial tests of this material displayed cracking through the deposit and rapid wear-through to the substrate, so this material could not be fairly evaluated and was eliminated from further testing.

4.5 Assessment of Surface Engineering Approaches for Ti-Alloys

A connecting rod big end bearing or other unidirectionally-moving component requires maintaining a regime of thick-film lubrication as much as possible to avoid solid contact and to enable the materials to withstand long periods of operation without excessive wear. If the majority of time of operation is spent with a well-established film of lubricant in the interface, then the materials need only sustain intermittent contact as the system starts up or shuts down. On the other hand, if the direction changes rapidly, as in a piston ring riding up and down a cylinder liner or the small end bearing of a connecting rod, then a stable lubricating film exists mainly during the mid-stroke portion of the cycle, and the materials play a more important role. The tests in Phase 1 were harder on the test materials than those in Phase 2 for that reason. Two of the surface treated Ti materials that failed Phase 1 (pin-on-flat tests) performed well in Phase 2 conditions (VLBT tests).

Consideration of the experimental data in the previous sections (reciprocating pin-on-flat (RPOF) versus unidirectionally rotating cylinder-on-flat (VLBT)) clearly demonstrates that a series of candidate materials can rank in a different order of merit when different friction and wear test methods are employed. In the case of reciprocating ball-on-flat tests, the contact pressure was in effect concentrated by the use of a spherical pin tip. Lubricant flow under such conditions also differed because flow around the sides and the direction of motion frequently reversed. Under the VLBT tests, the lubricant was fed into a converging wedge and the direction of motion of the test specimens was not reversed. Consequently, we screened the first series of candidate treatments (Section 4.2) in a different manner than the second set (Section 4.3-4). Results with respect to friction rankings are shown in Table 11.

Table 11.
Comparative Ranking of Surface Treatments by Two Different Tribo-Test Methods.

Flat Specimen Surface	**Phase 1: RPOF** (note 1)	**Phase 2: VLBT** (note 2)
High velocity powder consolidation (HVPC)	(note 3)	1
Carburized (Carb)	9 (note 4)	2
Chromium nitride coated (CrN)	**4**	**3**
Reference: CDA 932 (Brnz)	7	4
Titanium nitride coated (TiN)	5	5
Filled anodized layer (Anod)	12 (note 4)	6
Oxygen diffused (OD)	2	7
Nitrided (Nitr)	1	8
Ti alloy (Ti64)	11 (note 4)	9

Notes:
1) Ranked by lowest friction coefficient having the best ranking, and with greater than a friction coefficient of 0.15 considered 'failed.' Not all candidates from Phase 1 are listed because they were screened out prior to Phase 2. Therefore, some numbers are missing in the rank order
2) Ranked in considering both the lowest friction during the cycle, and the smallest range in friction coefficient (during a cycle than ranged from 30-100 N load)
3) The HVPC was not available for RPOF testing during Phase 1.
4) Did not pass Phase 1 criteria, but were tested in Phase 2 to determine if their behavior under different testing conditions would improve.

While the VLBT is probably a better simulation of a big end connecting rod bearing, the behavior of the various candidates to RPOF tests is a more rigorous test of the materials under boundary lubricated conditions. In that case, one needs to consider both results: the former as a well-lubricated test, and the latter as metric for transient, more severe conditions. From that point of view, the commercial CrN coating ranked high on both types of tests, although the HVPC coating also looks very attractive even though it was not tested under RPOF conditions in Phase 1.

Finally, these tests were conducted at ambient temperature. Conducting tests at engine temperatures could produce different results because: (1) the viscosity of the oil tends to decrease at elevated temperatures, leading to thinner fluid films and more solid contact, thus the role of materials properties would tend to become more important as temperature rises, (2) materials like the anodizing treatment with its polymer filler might not perform as well at elevated temperature due to filler softening, (3) the additives in formulated lubricating oils are activated by elevated temperatures and therefore, the chemical interactions, especially under boundary lubrication, could affect test results. It was found, for example, that the OD treatment for Ti favorably forms anti-wear films with formulated lubricating oils [19].

As a result of the foregoing discussion, certain additional lines of enquiry should be pursued:,

- Considering the leading candidates, what effects do elevated temperature and used oil have on tribological performance? This would require reconfiguring the VLBT for elevated temperature.

- How would the HVPC coatings that showed excellent friction and wear behavior under lubricated VLBT test conditions, perform under more severe wear conditions of boundary lubrication and sooty oil?

- In the present Phase 2 work, the sliding partner was 8620 steel and the lubricant a commercial diesel engine oil. The effects of using other counterface materials and lubricants should be investigated.

- One primary Ti alloy was the focus of this work (Ti-6Al-4V). It is possible that another Ti would be more amenable to the surface treatments than this one.

- Only one variant of each surface treatment was investigated in this work, yet it could be argued that the performance of a given treatment could be optimized for specific applications and substrates. Given the leading candidates identified here, a follow-on effort to optimize their performance could be conducted.

5.0 Publications

In addition to this final report, the following publications were produced:

1) D. G. Bansal, O. L. Eryilmaz, and P. J. Blau (2011) "Surface engineering to improve the durability and lubricity of Ti-6Al-4V alloy," *Wear*, Vol. 271, pp. 2006-2015. Also presented at the 2011 International Conference on Wear of Materials, April 2011, Philadelphia, PA.

2) D. G. Bansal, M. Kirkham, and P. J. Blau (2013 expected) "Effects of combined diffusion treatments and cold working on the sliding friction and wear behavior of Ti-6Al-4V," accepted for presentation at the 2013 International Conference on Wear of Materials, and publication in a special issue of the journal *Wear*.

3) P. J. Blau, K. M. Cooley, D. Bansal, I. Smid, T. J. Eden, M. Neshastehriz, J. K. Potter, and A. E. Segall (2013 expected) “Spectrum loading effects on the running-in of lubricated bronze and surface-treated titanium against alloy steel,” accepted for presentation at the 2013 International Conference on Wear of Materials, and publication in a special issue of the journal *Wear*.

6.0 Commercialization Possibilities

Several of the surface engineering approaches described here are commercially available thanks to prior investment by the defense and aerospace industry, but they have not been considered for components in diesel engines because titanium parts are not yet commonplace in heavy vehicle propulsion systems. The issue is whether the relevant engineering and cost factors alone would warrant such an investment. There is no question that Ti-alloys are lighter than steel and cast iron and there is no doubt that they are far more corrosion resistant as well.
Certain high-end performance vehicles, like the Porche 911 GT3 already use titanium connecting rods, however, in racing applications there are some concerns about fatigue life [20].

Therefore, the surface engineering technology investigated here under simulative conditions, if proven to perform well, could promote renewed consideration of Ti-alloys for fuel efficient diesel engines. Barring the highly unlikely probability of regulatory mandate requiring the use of Ti in engines, the following four issues will control its future introduction:

- Cost of the finished component, including raw materials, machining, and finishing
- Demonstrated equal or better performance to existing components
- Ease of integration/substitution of Ti alloy connecting rods and other bearing surface-containing parts into the engine designs, including the cost of developing manufacturing and quality control specifications for those new parts
- Availability and performance of existing lubricants with Ti-containing bearing surfaces

One of the contributors to the cost of Ti alloys in aerospace components has been the wastage of material during conventional manufacturing and finishing; however, the landscape of manufacturing has been changing in recent years to include innovative additive manufacturing processes that may reduce the cost of Ti components. One aspect of performance, the friction and wear of contact surfaces, was addressed here, but the integration of Ti alloys into design includes other properties like fatigue life, thermal expansion, and thermal conductivity (see Appendix C). For example, if a piston swells relative to the cylinder liner as it heats, there is a danger of scuffing or seizure. Therefore, the thermal behavior of the moving part must be considered in relationship to that that of the surrounding structures.

If durability and material compatibility issues can suitably be validated, fuel economy increases and ability to carry more load if the empty weight of a vehicle is reduced, then Ti could look better to the diesel engine community. Beyond that, friction and wear concerns for even the most promising candidate surface treatments will force designers to use inserts in a conservative, near-term approach in parts like connecting rod bearings.

7.0 Conclusions

The least risky course to further the use of lightweight, corrosion-resistant titanium alloy components as connecting rods, or other parts in which there is a need for repeated moving contact with another engine part, is to use inserts of conventional bearing materials rather than to attempt to treat or coat the surfaces of titanium itself.

Two types of friction and wear tests were used in this study of a variety of candidate coatings and surface treatments for Ti alloys. A ball-on-flat (point contact) reciprocating sliding test was used during the first phase of the effort to down-select candidates for the second phase. That test was hard on the materials, did not form a thick, stable lubricating film, and as a result produced relatively high friction coefficients typical of boundary lubrication or starved contact. The second type of test used unidirectional sliding with a cylinder-on-flat (line contact) which operated in low-friction regimes of lubrication in which the lubricant and surface finish seemed more relevant than the materials involved. In that regime, the materials did not make contact as often or with as much pressure. Not surprisingly, the candidate material choices ranked differently in the two test methods.

A satellite study of the effects of combined surface treatments, a mechanical treatment plus a diffusion treatment, showed little benefit under lubricant-starved test conditions, other than a temporary reduction in friction and wear for the first few meters of sliding. After that period, both treated surfaces showed the high friction and wear of the non-treated Ti alloy.

If the lubricant can be reliably supplied to maintain thick-film conditions during engine operation, then several of the Ti treatments and coatings could perform as well or better than a reference leaded bronze alloy. Two of the best candidates, based on the results of both types of screening tests, were a CrN commercial coating and a more experimental cold-sprayed Ni-B composite.

In summary, it would be prudent simply to avoid the use of titanium bearing surfaces entirely and use inserts of existing bearing materials in, for example, lightweight connecting rods. In less heavy-duty bearing surfaces, the results suggest limited future use of surface treated titanium for components that operate exclusively under mixed film or better, thick film lubrication conditions. Diffusion treatments like carburizing, nitriding, and oxygen diffusion treatments may provide limited protection for Ti, but are risky because once removed, the harsh friction and wear of titanium substrate occurs. A reasonable course could be to use a non-Ti, substrate durable hard coating such as CrN.

8.0 Cited References

1. P. J. Blau, B. C. Jolly, J. Qu, W. H. Peter, and C. A. Blue (2007) Tribological investigation of titanium-based materials for brakes," *Wear*, **Vol. 263**, pp. 1202-1211.

2. P. J. Blau (2007) *Prospects for Titanium-Based Materials as Truck Disc Brake Rotors*, ORNL Tech Report, ORNL TM-2007-111, 25 pp., available through OSTI.

3. M. G. Naylor, P. Kodali, and J. C. Wang (2001) Diesel Engine Tribology, Chapter 33 in Modern Tribology Handbook, Vol. 2, Ed. B. Bhushan, CRC Press, Boca Raton , pp. 1231-1269.

4. C. F. Taylor (1987) The Internal Combustion Engine in Theory and Practice, Vol. II, Combustion, Fuels, Materials, Design, MIT Press, Cambridge, MA, pp. 509-517.

5. Crankshaft Materials. Ref.: http://www.the-crankshaft.info/2009/07/crankshaft_06.html

6. R. Stribeck (1902) Die wesentlichen Eigenschaften der Gleit- und Rollenlager (The basic properties of sliding and rolling bearings), Zeitschrift des Vereins Deutscher Ingenieure, Nr. 36, Band 46, p. 1341-1348, 1432-1438, and 1463-1470.

7. M. Woydt and R. Wäsche (2010) The history of the Stribeck curve and ball bearing steels: The role of Adolf Martens, Wear, Vol. 268 (11-12), pp. 1542-1546.

8. P. S. Shenoy (2004) Dynamic Load Analysis and Optimization of Connecting Rod, reprint of an M.S. Thesis from the University of Toledo by the Iron and Steel Institute, Southfield, MI, 190 pp.

9. C. M. Taylor (1993) Engine Bearings: Background and Lubrication Analysis," Chapter 5 in Engine Tribology, ed. C. M. Taylor, Elsevier Pub., The Netherlands, pp. 89-112.

10. D.G. Bansal, O.L. Eryilmaz, P.J. Blau (2011) Surface engineering to improve the durability and lubricity of Ti-6Al-4V alloy, Wear, 271, pp. 2006-2015.

11 . D. G. Bansal, M. Kirkham, and P. J. Blau (2013 expected) Effects of combined diffusion treatments and cold working on the sliding friction and wear behavior of Ti-6Al-4V, accepted for the 19th International Conference on Wear of Materials, Portland, OR, April 14-18, 2013.

14. D. Balzar, N. Audebrand, M. R. Daymond, A. Fitch, A. Hewat, J. I. Langford, A. Le Bail, D. Louër, O. Masson, C. N. McCowan, N. C. Popa, P. W. Stephens, and B. H. Toby (2004) Size-strain line-broadening analysis of the ceria round-robin sample, Journal of Applied Crystallography, 37 (2004) 911–924.

12. ASTM G-133 (2011), Standard Test Method for Linearly Reciprocating Ball on Flat Sliding Wear, ASTM Annual Book of Standards, Vol. 03.02.

13. G. Shank, K. Goshorn, M. Cooper, W.V. Dam, S. Richards (2005) A History of Mack Engine Lubricant Tests from 1985-2005: Mack T-7 Through Mack T-12, in: SAE Transactions, SAE International, Warrendale, Pennsylvania, USA, 2005.

15. P. Scardi, M. Leoni, and R. Delhez (2004), Line broadening analysis using integral breadth methods: a critical review, Journal of Applied Crystallography, vol. 37, pp. 381–390

16. P. J. Blau, K. M. Cooley, D. Bansal, I. Smid, T. J. Eden, M. Neshastehriz, J. K. Potter, A. E. Segall (2013 – expected) "Spectrum loading effects on the running-in of lubricated bronze and surface-treated titanium against alloy steel, accepted for the 19th International Conference on Wear of Materials, Portland, OR, April 14-18, 2013.

17. J. Sun, X. Cai, and L. Liu (2010) Research on the Effect of Whole Cylinder Block on EHL Performance of Main Bearings Considering Crankshaft Deformation for Internal Combustion Engine, J. of Tribology, vol. 132, pp. 044502-1 to -6.

18. J. M. Ross and R. R. Slaymaker (1969) Journal Center Orbits in Piston Engine Bearings, Soc. of Automotive Engineers (SAE), paper number 690114.

19. J. Qu, P. J. Blau, J. Y. Howe, and H. M. Meyer, III (2009) Oxygen diffusion enables anti-wear boundary film formation on titanium surfaces in zinc-dialkyl-dithiophosphate (ZDDP)-containing lubricants, Scripta Materialia vol. 60, pp. 886–889.

20. R&R Racing Products, http://www.rrconnectingrods.com/how-to-choose-the-right-connecting-rod.html (2012).

9.0 Symbols and Nomenclature

Symbols

h	film thickness of a lubricant
σ_1	root-mean-square surface roughness of component 1
σ_o	composite surface roughness
μ	friction coefficient (see also CoF)
HRC	Rockwell hardness number (C scale)
HV	Vickers microindentation hardness number
P	applied (normal) load (also designated as *w* in film thickness calculations)
V	wear volume

Nomenclature

60NiTi	An alloy developed by NASA containing 60 wt.% NI and 40 wt. % Ti
Anod	Anodic surface filled with polymer used as a coating (see Tiodize™, Appendix A)
BB	(see Brnz)
Brnz	Bronze alloy CDA 932 (also referred to as 'BB' in some figures)
CR	Carburized surface treatment (also referred to as 'Carb')
Carb	(also referred to as "CR" in some figures and tables)
CoF	Coefficient of friction (see also μ)
CrN	Chromium nitride coating
CuNiIn	An electroplated coating of Cu, Ni, and In; often applied to connecting rod bearing inserts
DLC	Diamond coating (Note: This is not the usual designation for diamond coatings of this type but was used in this report for convenience in reporting.)
HVPC	High velocity powder consolidation coating
IR	Infrared melted composite surface layer containing Ti and TiB_2 particles
NAMB	Nanocomposite of Al, Mg, and B developed at Ames Laboratory in DOE-funded program.
NR	Nitrided surface treatment
Λ-ratio	in lubrication theory, the ratio of the lubricant film thickness to the composite roughness of the two facing bearing surfaces
OD	Oxygen diffusion treated surface
ORNL	Oak Ridge National Laboratory
PL	Planished surface
RPOF	Reciprocating pin-on-flat wear test method
SAE	Society of Automotive Engineers (sometimes uses as a designation for materials and specifications)
SP	Shot peened surface
Ti64	Alloy Ti-6 wt.%Al-4 wt. % V
TiN	Titanium nitride coated surface
VLBT	Variable load bearing test rig

Appendix A. Materials and Sources – Phase 1 Tests

The slider material in Phase 1 studies was a Cr-containing bearing steel AISI 52100 in the form of finished 9.53 mm diameter, Grade 10 balls. The following materials and surface treatments were used for the 25.4 × 25.4 × 6.3 mm thickness test coupons in this study. The designations in parentheses are used to identify the materials in subsequent discussions and data compilations. When multiple treatments are used, the designations are separated by a plus sign '+' in the order that the treatment was applied (i.e., treatment 1+ treatment 2).

Titanium alloy baseline material: Wrought, hot-rolled strip was purchased from a commercial source [A1], cut into test coupons without further heat treatment, and used for both substrate materials and for non-treated tests. The nominal composition of this material, according to ASTM B348-10, designated as Grade 5 titanium, in wt%, is: 5.5-6.75 Al, 3.5-4.5 V, 0.4 (max.) Fe, 0.20 (max.) O, 0.08 (max.) C, 0.05 (max.) N, 0.015 (max.) H, and balance Ti. The bulk hardness of the Ti64 specimens was 37.39 (±0.43) HRC.

Bearing bronze baseline material: Alloy CDA 932 is a popular leaded bronze alloy used in plain bearings for engines. It was obtained from a commercial source [A2] as bar stock and has the following typical composition in wt%: 6.3-7.5 Sn, 6.0-8.0 Pb,1.0-4.0 Zn, 0.35 Sb, 0.20 Fe, 1.0 Ni, 0.15 P, 0.08 S, 0.005 Si, 0.005 Al, and 83.0 (nominal) Cu. The alloy was tested in the as-received condition after surface finishing in successive steps to a 1.0 μm diamond lapped finish.

Nitinol: 60Ni-40Ti a NASA developed alloy was cast at Oak Ridge National Laboratory (ORNL). The bulk hardness of the as-cast alloy was 56.87 (±1.4) HRC, the high variation in the hardness measurement is due to the uneven cast surface of the alloy. In order to machine the alloy to the required dimensions, the specimen was heat treated as per a process recommended by Julien [A3]. This treatment consists of heating the specimen in a furnace at 700 ºC for 1 hour followed by gradual cooling in the furnace until the room temperature is reached. This reduces the bulk hardness to around 39.58 (±0.58) HRC, and makes the alloy amenable to machining or grinding and this version of the alloy is designated as **60NiTi**. The thickness of the oxide layer formed as a result of this heat treatment was around 7.4 μm. The test coupon was then polished sequentially with 400-grit, 600-grit and 1 μm diamond paste in the same order. Julien also recommended a subsequent heat treatment to harden the surface with a black oxide. This heat treatment involved heating the specimen in a furnace up to 945 ºC and holding it at that temperature for 15 minutes and then quenching it quickly in water. This covers the surface with a hard black colour oxide. The test coupon was then lightly polished with a 1 μm diamond paste. The bulk hardness increased to 41 (±0.59) HRC and this version of the alloy is designated as **60NiTi + HT**. The thickness of the oxide layer formed as a result of this heat treatment was around 10 μm, resulting in a total oxide thickness of around 17−18 μm.

Oxygen-diffused Ti64 : The Ti64 base material was used as the substrate for an oxygen diffusion treatment consisting of exposure to 800 ºC in air for two hours, followed by an air cool [A4]. Loose surface scales were lightly abraded away with 600 grit sand paper to produce a smooth surface with an enriched oxygen subsurface zone approximately 20 μm thick.

Nitrided Ti64: The nitriding of the Ti64 test coupons was performed by Solar Atmospheres [A5]. The furnace was pump down into hard vacuum (below 5×10^{-4} torr) to start the cycle with a very low oxygen atmosphere. The furnace was then slowly ramped to 800 °C (+0°/-14 °C). This was followed with introduction of a partial pressure of nitrogen gas with a constant flow rate through the furnace, in order to maintain a dynamic atmosphere. The furnace was held at that temperature for two hours and quenched with a nitrogen gas backfill and internal furnace blower fan.

Carburized Ti64: The carburizing of the Ti64 test coupons was performed by Solar Atmospheres [A5]. The furnace vacuum and the ramp up were same as that for the nitriding process. The carburizing gas used was acetylene. A total of 21 boost/diffuse sequences were used for a total cycle time of seven hours. The boost was in a partial pressure of acetylene and the diffusion in a partial pressure of argon. The boosts become shorter in time and the diffusion longer as the cycle progresses. The furnace was cooled with an argon gas backfill and internal furnace blower fan at the end of the cycle.

Microcomposite by infrared surface processing: A novel, infrared surface treatment was used to produce Ti matrix composite coating deposits approximately 300 to 500 µm thick, containing micrometer-sized hard particles. They were prepared by rapid surface melting of mixed powders (Ti64 plus approximately 25% by volume of -100 mesh TiB_2 powder) using a Vortek™ plasma arc lamp. The lamp is a direct current, water-wall-stabilized, high-pressure argon arc lamp with a maximum power of 300 kW at an arc current of 1000 A. The heating was conducted in a water cooled box with flowing argon gas. The arc lamp was configured with a 35 cm long parabolic reflector to create line source heating with a half intensity width of about 1 cm. Powder coated samples were traversed at 6 to 7 mm/s in two passes, a preheat pass at 600 to 700 A, followed immediately by a melt pass at 875 to 900 A. Prior to IR treatment, powder blends were first mixed into an aqueous solution with a polymer binder. The suspended powder particles were then sprayed onto pre-weighed plates of Ti-6Al-4 V, dried in air for 12 hours, and heated to 650 ºC to remove the remaining binder. The test specimen was exposed to 485 ºC in air for approximately 3 hrs after polishing, and as a result had a thin layer of oxide.

Nanocomposite coating containing Al-Mg-B / TiB_2: This coating material was developed by Ames Laboratory and Eaton Corporation under a research contract sponsored by the U.S. Department of Energy, Industrial Technologies Program. With a thickness of approximately 4−5 mm, it is produced by a multiple electrode chamber deposition process with a thin carbon layer [A6]. This coating was selected based on prior experience on a different research project on advanced coating materials.

Shot peening Ti64 : The test surfaces of the coupons were shot peened with the following parameters, 230H cast shot with 0.008-0.012" A (Almen intensity) and coverage of 125%. The same parameters were used for shot peening oxygen diffusion treated Ti64 coupons (OD + SP), nitrided Ti64 coupons (NR + SP) and carburized Ti64 coupons (CR + SP). Shot peening was performed by Metal Improvement Company, Milwaukee WI [A7].

TiN coating: TiN coating on Ti64 coupons was provided by Phygen Coatings Inc. [A8]. The coating thickness was in the range of 3−4 µm.

Chromium nitride coating: CrN or FortiPhy™ coating on Ti64 coupons was provided by Phygen Coatings Inc.[A8] using their patented physical vapor deposition process. The coating thickness was around 3 µm.

Diamond films: The nearly frictionless diamond-like-carbon coatings, provided by Argonne National Laboratory (ANL), were grown from pure CH_4 by using a plasma enhanced chemical vapor depositions (PE-CVD) technique [A9-A11]. The coating thickness was in the range of 1−1.4 µm.

Cu-Ni-In coating: The bearing bronze and Ti64 test coupons were coated with Cu-Ni-In using a thermal spray process. The coating was performed by Ellison Surface Technologies [A12] using their proprietary composition and process parameters. The coating thickness was in the range of 30 − 34 µm.

Anodizing: TIODIZE, an anodizing process for titanium, was performed by TIODIZE Technologies [A13]. The TIODIZE IV process involves impregnating TIOLON X40 PTFE into the surface to provide low friction and anti-galling for longer life at higher loads. This process was selected from an internet search of coating processes for titanium. According to TIODIZE Technologies, this process prevents the failure due to galling and reduces the coefficient of friction.

Appendix References

[A1] Grade 5 titanium strip, McMaster Carr Supply, Atlanta, Georgia

[A2] Atlas Bronze, Trenton, NJ

[A3] G.J. Julien, Nitinol ball bearing element and process for making in: U.S. Patent No. 6886986, Nitinol Technologies Inc., USA, 2005.

[A4] J. Qu, P.J. Blau, J.Y. Howe, H.M. Meyer Iii, Oxygen diffusion enables anti-wear boundary film formation on titanium surfaces in zinc-dialkyl-dithiophosphate (ZDDP)-containing lubricants, Scripta Materialia, 60 (2009) 886-889.

[A5] Solar Atmospheres, Souderton, PA.

[A6] Courtesy of the Eaton Innovation Center, Southfield, MI

[A7] Metal Improvement Company, Milwaukee WI

[A8] Courtesy of Phygen Coatings Inc., Minneapolis, MN

[A9] A. Erdemir, I.B. Nilufer, O.L. Eryilmaz, M. Beschliesser, G.R. Fenske, Friction and wear performance of diamond-like carbon films grown in various source gas plasmas, in: 26th International Conference on Metallurgical Coatings and Thin Films, 12-15 April 1999, Elsevier, Switzerland, 1999, pp. 589-593.

[A10] A. Erdemir, O.L. Eryilmaz, I.B. Nilufer, G.R. Fenske, Synthesis of superlow-friction carbon films from highly hydrogenated methane plasmas, Surface and Coatings Technology, 133-134 (2000) 448-454.

[A11] A. Erdemir, O.L. Eryilmaz, I.B. Nilufer, G.R. Fenske, Effect of source gas chemistry on tribological performance of diamond-like carbon films, in: 10th European Conference on Diamond, Diamond-like Materials, Carbon Nanotubes, Nitrides and Silicon Carbide, September 12, 1999 - September 17, 1999, Elsevier S.A., Prague, Czech Republic, 2000, pp. 632-637.

[A12] Ellison Surface Technologies, Mason OH

[A13] TIODIZE Technologies, Huntington Beach, CA

Appendix B. Table of VLBT Data for Cycle 10 of Spectrum Tests

VLBT#	25			VLBT#	28			VLBT#	29			VLBT#	30		
SURFACE	**Bare CDA 932 Bronze**			SURFACE	**Bare CDA 932 Bronze**			SURFACE	**Non-treated Ti-6Al-4V**			SURFACE	**Non-treated Ti-6Al-4V**		
		Ave COF	**0.019**			Ave COF	**0.016**			Ave COF	**0.234**			Ave COF	**0.238**
		StdDev	**0.001**			StdDev	**0.002**			StdDev	**0.042**			StdDev	**0.043**
		Max COF	**0.020**			Max COF	**0.019**			Max COF	**0.300**			Max COF	**0.307**
		Min COF	0.017			Min COF	0.014			Min COF	0.115			Min COF	0.123
Time	Load, P	1/P	Fric Coeff	Time	Load, P	1/P	Fric Coeff	Time	Load, P	1/P	Fric Coeff	Time	Load, P	1/P	Fric Coeff
(s)	(N)	(N^-1)	(n/d)	(s)	(N)	(N^-1)	(n/d)	(s)	(N)	(N^-1)	(n/d)	(s)	(N)	(N^-1)	(n/d)
1082	31.07	0.032185	0.02	1080.017	54.31507	0.018411	0.016675	1086	29.67	0.033704	0.188	1082.022	33.72528	0.029651	0.241128
1084	30.98	0.032279	0.019	1082.019	35.00508	0.028567	0.014563	1088	29.81	0.033546	0.176	1084.023	29.67837	0.033695	0.23013
1086	31.12	0.032134	0.019	1084.017	30.71728	0.032555	0.014247	1090	29.71	0.033659	0.158	1086.024	29.71324	0.033655	0.208636
1088	30.96	0.0323	0.019	1086.018	30.67299	0.032602	0.014439	1092	29.78	0.03358	0.153	1088.023	29.66233	0.033713	0.175767
1090	30.95	0.03231	0.019	1088.019	30.78417	0.032484	0.013658	1094	29.89	0.033456	0.148	1090.024	29.762	0.0336	0.160862
1092	31	0.032258	0.019	1090.019	30.90003	0.032362	0.014637	1096	29.74	0.033625	0.143	1092.015	29.71663	0.033651	0.157116
1094	30.97	0.032289	0.02	1092.012	30.95183	0.032308	0.013926	1098	29.76	0.033602	0.125	1094.025	29.59632	0.033788	0.146446
1096	31.07	0.032185	0.018	1094.018	30.86226	0.032402	0.014043	1100	29.75	0.033613	0.115	1096.023	29.66279	0.033712	0.141697
1098	31.07	0.032185	0.019	1096.017	30.84146	0.032424	0.015219	1102	49.59	0.020165	0.168	1098.023	29.62941	0.03375	0.140945
1100	50.75	0.019704	0.018	1098.018	30.91007	0.032352	0.014267	1104	53.74	0.018608	0.191	1100.022	29.71996	0.033647	0.123311
1102	54.74	0.018268	0.018	1100.018	30.83201	0.032434	0.01425	1106	53.8	0.018587	0.195	1102.021	49.24367	0.020307	0.169281
1104	54.75	0.018265	0.018	1102.018	50.32323	0.019872	0.016469	1108	53.52	0.018685	0.211	1104.025	53.39136	0.01873	0.192065
1106	54.71	0.018278	0.018	1104.018	54.77267	0.018257	0.016875	1110	53.74	0.018608	0.211	1106.023	53.51514	0.018686	0.200783
1108	54.25	0.018433	0.018	1106.018	54.69685	0.018283	0.016213	1112	71.25	0.014035	0.214	1108.023	53.40669	0.018724	0.204983
1110	72.38	0.013816	0.019	1108.018	54.57456	0.018324	0.016918	1114	74.62	0.013401	0.235	1110.022	53.42701	0.018717	0.209747
1112	75.91	0.013173	0.019	1110.018	54.71688	0.018276	0.017392	1116	74.62	0.013401	0.249	1112.023	71.10868	0.014063	0.22691
1114	75.98	0.013161	0.019	1112.018	72.13467	0.013863	0.017949	1118	74.6	0.013405	0.248	1114.026	74.42363	0.013437	0.247952
1116	76.02	0.013154	0.019	1114.019	75.81154	0.013191	0.018437	1120	74.62	0.013401	0.252	1116.023	74.53645	0.013416	0.260201
1118	75.95	0.013167	0.019	1116.018	75.68039	0.013213	0.018365	1122	49.53	0.02019	0.266	1118.022	74.39841	0.013441	0.26265
1120	50.85	0.019666	0.018	1118.019	75.66412	0.013216	0.018012	1124	43.4	0.023041	0.264	1120.022	74.39132	0.013442	0.272374
1122	44.64	0.022401	0.019	1120.018	75.73618	0.013204	0.018048	1126	43.49	0.022994	0.251	1122.024	49.31407	0.020278	0.30647
1124	44.69	0.022376	0.019	1120.018	75.73618	0.013204	0.018048	1128	43.51	0.022983	0.233	1124.023	43.2914	0.023099	0.26574
1126	44.51	0.022467	0.019	1122.019	50.54711	0.019784	0.016312	1130	43.53	0.022973	0.227	1126.024	43.33505	0.023076	0.238486
1128	44.74	0.022351	0.02	1124.017	44.51286	0.022465	0.015579	1132	43.4	0.023041	0.221	1128.023	43.18522	0.023156	0.218017
1130	44.73	0.022356	0.019	1126.019	44.67845	0.022382	0.015067	1134	43.31	0.023089	0.208	1130.023	43.10038	0.023202	0.220202
1132	44.73	0.022356	0.018	1128.017	44.57591	0.022434	0.015411	1136	51.72	0.019335	0.205	1132.024	43.28695	0.023102	0.217108
1134	53.04	0.018854	0.019	1130.017	44.51191	0.022466	0.015128	1138	69.29	0.014432	0.237	1134.024	43.26354	0.023114	0.212379
1136	70.57	0.01417	0.019	1132.018	44.51039	0.022467	0.015461	1140	69.34	0.014422	0.248	1136.023	50.97638	0.019617	0.206354
1138	70.62	0.01416	0.019	1134.02	44.45712	0.022494	0.015687	1142	69.41	0.014407	0.253	1138.023	69.03874	0.014485	0.234684
1140	70.69	0.014146	0.019	1136.02	53.16291	0.01881	0.016788	1144	69.45	0.014399	0.257	1140.023	69.03461	0.014485	0.249543
1142	70.46	0.014192	0.019	1138.019	70.13963	0.014257	0.017915	1146	78.15	0.012796	0.239	1142.024	69.15058	0.014461	0.254846
1144	80.1	0.012484	0.018	1140.018	70.39456	0.014206	0.017666	1148	96.57	0.010355	0.235	1144.044	69.12107	0.014467	0.259577
1146	101.83	0.00982	0.02	1142.021	70.38704	0.014207	0.01752	1150	96.52	0.010361	0.249	1146.023	78.09868	0.012804	0.255782
1148	101.68	0.009835	0.019	1144.018	70.27417	0.01423	0.01796	1152	96.51	0.010362	0.251	1148.023	97.00654	0.010309	0.247731
1150	101.43	0.009859	0.019	1146.017	80.74118	0.012385	0.018491	1154	96.56	0.010356	0.256	1150.024	96.744	0.010337	0.253429
1152	101.76	0.009827	0.019	1148.018	102.7083	0.009736	0.018916	1156	87.26	0.01146	0.274	1152.022	97.168	0.010291	0.26126
1154	90.89	0.011002	0.019	1150.017	101.9902	0.009805	0.018632	1158	69.19	0.014453	0.3	1154.023	97.00852	0.010308	0.263862
1156	70.13	0.014259	0.018	1152.018	102.0557	0.009799	0.018586	1160	69.19	0.014453	0.285	1156.025	87.5245	0.011425	0.281239
1158	70.37	0.014211	0.019	1154.02	101.6316	0.009839	0.018348	1162	69.02	0.014489	0.279	1158.022	68.80226	0.014534	0.306571
1160	70.39	0.014207	0.018	1156.02	90.97183	0.010992	0.018214	1164	69.01	0.014491	0.281	1160.024	68.83314	0.014528	0.305386
1162	70.44	0.014196	0.018	1158.018	70.18256	0.014249	0.016488	1166	60.87	0.016428	0.291	1162.024	68.74274	0.014547	0.294789
1164	61.9	0.016155	0.019	1160.018	70.0428	0.014277	0.016446	1168	43.31	0.023089	0.287	1164.026	68.92337	0.014509	0.284747
1166	44.59	0.022427	0.018	1162.017	69.89147	0.014308	0.017008	1170	43.28	0.023105	0.283	1166.023	60.51005	0.016526	0.283091
1168	44.59	0.022427	0.018	1164.019	70.08349	0.014269	0.016924	1172	43.33	0.023079	0.267	1168.026	43.1236	0.023189	0.289872
1170	44.63	0.022406	0.018	1166.018	61.69962	0.016208	0.016316	1174	43.26	0.023116	0.265	1170.025	43.11212	0.023195	0.275513
1172	44.65	0.022396	0.018	1168.017	44.23261	0.022608	0.014505	1176	43.22	0.023137	0.253	1172.024	43.09533	0.023204	0.257795
1174	44.59	0.022427	0.018	1170.018	44.24054	0.022604	0.014812	1178	43.27	0.023111	0.245	1174.025	43.098	0.023203	0.239938
1176	44.62	0.022411	0.018	1172.018	44.31245	0.022567	0.014787	1180	43.2	0.023148	0.247	1176.025	43.19205	0.023152	0.225532
1178	44.57	0.022437	0.017	1174.018	44.40555	0.02252	0.014882	1182	67.8	0.014749	0.242	1178.024	43.14329	0.023179	0.223932
1180	69.73	0.014341	0.018	1176.02	44.52009	0.022462	0.014561	1184	74.43	0.013435	0.255	1180.023	43.14272	0.023179	0.221014
1182	75.79	0.013194	0.018	1178.019	44.48648	0.022479	0.014578	1186	74.46	0.01343	0.263	1182.023	68.46583	0.014606	0.241074
1184	75.86	0.013182	0.019	1180.019	44.40696	0.022519	0.015176	1188	74.65	0.013396	0.265	1184.025	74.24401	0.013469	0.261477
1186	76.82	0.013017	0.018	1182.018	69.43982	0.014401	0.017282	1190	74.64	0.013398	0.263	1186.024	74.35407	0.013449	0.263402
1188	75.74	0.013203	0.019	1184.02	75.39303	0.013264	0.017815	1192	56.73	0.017627	0.271	1188.024	74.28267	0.013462	0.272689
1190	57.9	0.017271	0.018	1186.017	75.5618	0.013234	0.018014	1194	53.31	0.018758	0.259	1190.023	74.26387	0.013465	0.270728
1192	54.49	0.018352	0.018	1188.02	75.43562	0.013256	0.017578	1196	53.29	0.018765	0.255	1190.023	74.26387	0.013465	0.270728
1194	54.53	0.018339	0.019	1190.018	75.29809	0.013281	0.017998	1198	53.35	0.018744	0.246	1192.024	56.53599	0.017688	0.285236
1196	54.49	0.018352	0.017	1190.018	75.29809	0.013281	0.017998	1200	53.33	0.018751	0.252	1194.027	52.94278	0.018888	0.273603
1198	34.76	0.028769	0.018	1192.019	57.55382	0.017375	0.016494	1202	33.89	0.029507	0.242	1196.025	52.93773	0.01889	0.256123
1200	34.76	0.028769	0.02	1194.02	54.38162	0.018389	0.016051	1204	29.87	0.033478	0.217	1198.025	53.0475	0.018851	0.248652
1202	31.11	0.032144	0.018	1196.018	54.41531	0.018377	0.016061	1206	29.84	0.033512	0.199	1200.023	52.95205	0.018885	0.243862
1204	30.93	0.032331	0.019	1198.019	54.36067	0.018396	0.016774					1202.023	33.88938	0.029508	0.246888
1206	31.14	0.032113	0.019	1200.018	54.34856	0.0184	0.01607					1204.024	29.6328	0.033746	0.21497

VLBT#	35			VLBT#	36			VLBT#	39			VLBT#	40		
SURFACE	**OD - Ti-6Al-4V**			SURFACE	**OD - Ti-6Al-4V**			SURFACE	**Nitrided Ti-6Al-4V**			SURFACE	**Nitrided Ti-6Al-4V**		
		Ave COF	**0.021**			Ave COF	**0.040**			Ave COF	**0.029**			Ave COF	**0.025**
		StdDev	**0.006**			StdDev	**0.004**			StdDev	**0.013**			StdDev	**0.010**
		Max COF	**0.035**			Max COF	**0.052**			Max COF	**0.066**			Max COF	**0.048**
		Min COF	0.013			Min COF	0.033			Min COF	0.015			Min COF	0.011
Time	Load, P	1/P	Fric Coeff	Time	Load, P	1/P	Fric Coeff	Time	Load, P	1/P	Fric Coeff	Time	Load, P	1/P	Fric Coeff
(s)	(N)	(N^-1)	(n/d)	(s)	(N)	(N^-1)	(n/d)	(s)	(N)	(N^-1)	(n/d)	(s)	(N)	(N^-1)	(n/d)
1082.022	32.68128	0.030599	0.014817	1086.023	32.14721	0.031107	0.034859	1082.022	36.44802	0.027436	0.015754	1082.014	32.33005	0.030931	0.011164
1082.022	32.68128	0.030599	0.014817	1088.023	32.08427	0.031168	0.036507	1084.021	36.35966	0.027503	0.015302	1084.015	32.37649	0.030887	0.01142
1084.023	32.47454	0.030793	0.014497	1090.024	32.07922	0.031173	0.035998	1086.023	36.43872	0.027443	0.015155	1086.015	32.31832	0.030942	0.011533
1086.022	32.46952	0.030798	0.014418	1094.038	31.95783	0.031291	0.036328	1088.023	36.38382	0.027485	0.015356	1088.015	32.39798	0.030866	0.012029
1088.023	32.54115	0.03073	0.014987	1096.024	32.11403	0.031139	0.0355	1090.008	36.37335	0.027493	0.015681	1090.006	32.33031	0.030931	0.011175
1090.013	32.52654	0.030744	0.014542	1098.023	32.15166	0.031103	0.036412	1092.034	36.34672	0.027513	0.015569	1092.016	32.14839	0.031106	0.011041
1092.022	32.4583	0.030809	0.014859	1100.023	32.05064	0.031201	0.036416	1094.021	36.47741	0.027414	0.015029	1094.015	32.42307	0.030842	0.01242
1094.024	32.6397	0.030638	0.014211	1102.024	51.54025	0.019402	0.039536	1096.02	36.49581	0.0274	0.015924	1096.016	32.45954	0.030808	0.011262
1096.023	32.62142	0.030655	0.013488	1104.023	55.95392	0.017872	0.040217	1098.023	36.35564	0.027506	0.015181	1098.017	32.39847	0.030866	0.011275
1098.023	32.65471	0.030623	0.013661	1106.023	55.98188	0.017863	0.039862	1100.021	57.11726	0.017508	0.026829	1100.015	52.60001	0.019011	0.023093
1100.023	52.27656	0.019129	0.018083	1108.024	56.09561	0.017827	0.039814	1102.021	61.38394	0.016291	0.027465	1102.014	57.52214	0.017385	0.025562
1102.022	56.49956	0.017699	0.017648	1110.025	56.05704	0.017839	0.040179	1104.041	61.44756	0.016274	0.027992	1104.016	57.14377	0.0175	0.025557
1104.021	56.62288	0.017661	0.018243	1112.023	73.4872	0.013608	0.04143	1106.023	61.24429	0.016328	0.027707	1106.016	57.29789	0.017453	0.025382
1106.023	56.61843	0.017662	0.018724	1114.024	77.19759	0.012954	0.042099	1108.023	61.45531	0.016272	0.02768	1108.014	57.22657	0.017474	0.026048
1108.023	56.73971	0.017624	0.017771	1116.024	77.04603	0.012979	0.04301	1110.022	78.32798	0.012767	0.033451	1110.015	74.66336	0.013393	0.03074
1110.023	74.29288	0.01346	0.024666	1118.023	77.20376	0.012953	0.042252	1112.021	81.8064	0.012224	0.033913	1112.015	77.75561	0.012861	0.031822
1112.023	77.65673	0.012877	0.025381	1120.023	76.99791	0.012987	0.043072	1114.021	81.89651	0.012211	0.034305	1114.015	77.85881	0.012844	0.031634
1114.024	77.78619	0.012856	0.025531	1122.023	51.52668	0.019407	0.040741	1116.02	81.8481	0.012218	0.034268	1116.014	77.7369	0.012864	0.031689
1116.023	77.8008	0.012853	0.025766	1124.023	45.75903	0.021854	0.039031	1118.021	81.94134	0.012204	0.033992	1118.016	77.80977	0.012852	0.031876
1118.023	77.69622	0.012871	0.024861	1126.022	45.59728	0.021931	0.03763	1120.023	56.64511	0.017654	0.025053	1120.015	52.37539	0.019093	0.022932
1120.022	52.47568	0.019056	0.018855	1126.022	45.59728	0.021931	0.03763	1122.022	50.42936	0.01983	0.021739	1122.015	46.37376	0.021564	0.020036
1122.022	46.54889	0.021483	0.01705	1128.026	45.64119	0.02191	0.039297	1124.032	50.49663	0.019803	0.022264	1124.015	46.30936	0.021594	0.019497
1124.023	46.41355	0.021545	0.016998	1130.023	45.83141	0.021819	0.038216	1126.022	50.45146	0.019821	0.02219	1126.015	46.29619	0.0216	0.019506
1126.02	46.33733	0.021581	0.016917	1132.023	45.6391	0.021911	0.037145	1128.022	50.36539	0.019855	0.022041	1128.015	46.16213	0.021663	0.020099
1128.023	46.44139	0.021533	0.01586	1134.024	45.69093	0.021886	0.038241	1130.038	50.49296	0.019805	0.022315	1130.015	46.2645	0.021615	0.019711
1130.023	46.36267	0.021569	0.016879	1136.024	53.92846	0.018543	0.038424	1132.022	50.39719	0.019842	0.021956	1132.015	46.17531	0.021657	0.019354
1132.024	46.23218	0.02163	0.017238	1138.023	71.75753	0.013936	0.040652	1134.022	59.19848	0.016892	0.026929	1134.015	54.75978	0.018262	0.02463
1134.024	54.70031	0.018281	0.019481	1140.024	71.71107	0.013945	0.040821	1136.023	76.75406	0.013029	0.032418	1136.015	72.68907	0.013757	0.030838
1136.022	72.4112	0.01381	0.023699	1142.023	71.74296	0.013939	0.040669	1138.021	76.69695	0.013038	0.032581	1138.017	72.45182	0.013802	0.030823
1138.023	72.24518	0.013842	0.023135	1144.037	71.70364	0.013946	0.04072	1140.022	76.56066	0.013062	0.032603	1140.017	72.40205	0.013812	0.030609
1140.023	72.41711	0.013809	0.023697	1146.026	80.85754	0.012367	0.044614	1142.022	76.66105	0.013044	0.032386	1142.017	72.46221	0.0138	0.030543
1142.022	72.33552	0.013824	0.023301	1148.023	103.3555	0.009675	0.051145	1144.022	106.1533	0.00942	0.046761	1144.016	89.88111	0.011126	0.036328
1144.023	82.44334	0.01213	0.027468	1150.025	102.6997	0.009737	0.05174	1146.023	188.0089	0.005319	0.063907	1146.015	154.0014	0.006493	0.047549
1146.025	107.8596	0.009271	0.035211	1152.024	103.1217	0.009697	0.051539	1148.023	188.0089	0.005319	0.064822	1148.015	153.927	0.006497	0.047977
1148.024	106.296	0.009408	0.034685	1154.024	103.0465	0.009704	0.051488	1150.021	188.0089	0.005319	0.065896	1150.014	153.8767	0.006499	0.048064
1150.022	105.3917	0.009488	0.034667	1156.022	92.48605	0.010812	0.048269	1152.022	188.0089	0.005319	0.066199	1152.015	150.6519	0.006638	0.047898
1152.025	104.4584	0.009573	0.03466	1158.023	71.64337	0.013958	0.040964	1154.022	143.9854	0.006945	0.060215	1154.014	117.0945	0.00854	0.042759
1154.023	94.762	0.010553	0.032589	1160.024	71.45651	0.013995	0.041207	1156.024	75.71861	0.013207	0.032694	1156.038	70.97123	0.01409	0.029455
1156.024	72.24147	0.013842	0.024112	1162.024	71.57768	0.013971	0.040373	1158.035	75.86101	0.013182	0.032748	1158.016	70.74485	0.014135	0.029594
1158.023	72.25356	0.01384	0.023778	1164.023	71.53871	0.013978	0.039324	1160.022	75.67465	0.013214	0.032755	1160.017	71.18638	0.014048	0.029154
1160.022	72.18738	0.013853	0.023614	1164.023	71.53871	0.013978	0.039324	1162.023	75.79131	0.013194	0.032845	1162.017	71.04335	0.014076	0.029682
1162.023	72.30438	0.01383	0.023887	1166.035	63.24458	0.015812	0.039592	1164.032	67.59045	0.014795	0.030611	1164.015	62.97906	0.015878	0.026994
1164.024	63.94046	0.01564	0.022078	1168.024	45.46645	0.021994	0.038744	1166.023	50.55833	0.019779	0.022732	1166.015	46.157	0.021665	0.020242
1166.024	46.20296	0.021644	0.017192	1170.024	45.62911	0.021916	0.037228	1168.024	50.59056	0.019767	0.023027	1168.016	46.09598	0.021694	0.02061
1168.024	46.28323	0.021606	0.015962	1172.023	45.53466	0.021961	0.035719	1170.037	50.76611	0.019698	0.023559	1170.016	46.22656	0.021633	0.020001
1170.024	46.21484	0.021638	0.01628	1174.021	45.59123	0.021934	0.037535	1172.022	50.60999	0.019759	0.023121	1172.015	46.27383	0.02161	0.020271
1172.024	46.22902	0.021631	0.017145	1176.023	45.57963	0.02194	0.036652	1174.023	50.69023	0.019728	0.023594	1174.016	46.12761	0.021679	0.020131
1174.042	46.2378	0.021627	0.016653	1178.024	45.47325	0.021991	0.037683	1176.023	50.56246	0.019778	0.022973	1176.015	46.17344	0.021657	0.020245
1176.024	46.07517	0.021704	0.016426	1180.025	45.61166	0.021924	0.03786	1178.023	50.79389	0.019687	0.022981	1178.017	46.27687	0.021609	0.020358
1178.022	46.14907	0.021669	0.016674	1182.025	71.02047	0.01408	0.040553	1180.023	75.88415	0.013178	0.033404	1180.016	71.41373	0.014003	0.030389
1180.022	71.52166	0.013982	0.02398	1184.024	77.03926	0.01298	0.041112	1182.023	81.83372	0.01222	0.034783	1182.016	77.65063	0.012878	0.031771
1182.023	77.56774	0.012892	0.025644	1186.025	77.0652	0.012976	0.041681	1184.022	81.93824	0.012204	0.035071	1184.014	77.51483	0.012901	0.031776
1184.022	77.5707	0.012891	0.026088	1188.024	77.01292	0.012985	0.04127	1186.022	81.71459	0.012238	0.034647	1186.015	77.68209	0.012873	0.031891
1186.023	77.71138	0.012868	0.025982	1192.023	59.15061	0.016906	0.038644	1188.022	81.96329	0.012201	0.034973	1188.015	77.48401	0.012906	0.032426
1188.022	77.6747	0.012874	0.025423	1194.023	55.7809	0.017927	0.03816	1190.022	63.26685	0.015806	0.028632	1190.018	59.17469	0.016899	0.026209
1190.03	59.84511	0.01671	0.019382	1196.024	55.56291	0.017998	0.038989	1192.023	59.9775	0.016673	0.02705	1192.017	55.56159	0.017998	0.024647
1192.023	56.29572	0.017763	0.018506	1198.023	55.61364	0.017981	0.038732	1194.023	60.10487	0.016638	0.027094	1194.017	55.48924	0.018022	0.024256
1194.024	56.18973	0.017797	0.01796	1200.025	55.84303	0.017907	0.038097	1196.021	60.05338	0.016652	0.02748	1196.017	55.57755	0.017993	0.024066
1196.025	56.29707	0.017763	0.018414	1202.024	36.49861	0.027398	0.035578	1198.023	60.00824	0.016664	0.027059	1198.017	55.5384	0.018006	0.024403
1198.022	56.39114	0.017733	0.01863	1204.025	31.95605	0.031293	0.036082	1200.023	40.49163	0.024696	0.017973	1200.016	36.15231	0.027661	0.015685
1200.038	36.45498	0.027431	0.016465	1206.024	32.101	0.031152	0.032628	1202.022	36.2486	0.027587	0.015705	1202.016	32.30873	0.030951	0.011203
1202.049	32.67477	0.030605	0.016403					1204.021	36.37728	0.02749	0.016678	1204.016	32.20728	0.031049	0.011568
1204.024	32.65155	0.030626	0.016629					1206.024	36.32473	0.027529	0.015734	1206.014	32.39224	0.030872	0.012227

VLBT#	**41**			VLBT#	**42**			VLBT#	**43**			VLBT#	**44**		
SURFACE	**TiN coated Ti-6Al-4V**			SURFACE	**TiN coated Ti-6Al-4V**			SURFACE	**CrN (Fortiphy TM)**			SURFACE	**CrN (Fortiphy TM)**		
		Ave COF	**0.012**			Ave COF	**0.016**			Ave COF	**0.014**			Ave COF	**0.011**
		StdDev	**0.005**			StdDev	**0.004**			StdDev	**0.006**			StdDev	**0.003**
		Max COF	**0.027**			Max COF	**0.029**			Max COF	**0.035**			Max COF	**0.020**
		Min COF	0.008			Min COF	0.011			Min COF	0.009			Min COF	0.008
Time	Load, P	1/P	Fric Coeff	Time	Load, P	1/P	Fric Coeff	Time	Load, P	1/P	Fric Coeff	Time	Load, P	1/P	Fric Coeff
(s)	(N)	(N^-1)	(n/d)	(s)	(N)	(N^-1)	(n/d)	(s)	(N)	(N^-1)	(n/d)	(s)	(N)	(N^-1)	(n/d)
1080.024	36.02016	0.027762	0.008743	1082.024	31.93208	0.031316	0.010519	1080.023	42.59227	0.023478	0.011505	1082.023	34.16436	0.02927	0.010985
1082.023	31.76645	0.03148	0.008732	1084.023	31.94565	0.031303	0.011091	1082.022	38.62176	0.025892	0.01221	1084.022	34.20026	0.02924	0.010282
1084.022	31.82689	0.03142	0.008588	1086.024	31.90415	0.031344	0.011575	1084.02	38.32404	0.026093	0.011732	1086.021	34.13336	0.029297	0.010585
1086.022	32.10108	0.031152	0.009218	1088.024	31.86693	0.03138	0.011001	1086.023	38.36674	0.026064	0.011875	1088.022	34.1616	0.029273	0.010459
1088.022	31.96008	0.031289	0.008725	1090.02	31.88071	0.031367	0.011924	1088.023	38.39444	0.026045	0.012365	1090.011	34.17948	0.029257	0.011137
1090.014	31.93362	0.031315	0.008287	1092.023	32.16462	0.03109	0.011158	1090.013	38.41378	0.026032	0.012135	1092.023	34.13835	0.029293	0.01063
1092.024	32.19685	0.031059	0.008628	1094.023	31.97828	0.031271	0.011567	1092.022	38.36293	0.026067	0.012348	1094.023	34.29522	0.029159	0.011142
1094.024	31.92082	0.031328	0.008536	1096.023	31.86753	0.03138	0.011044	1094.023	38.38184	0.026054	0.012781	1096.022	34.1969	0.029242	0.01037
1096.025	31.95589	0.031293	0.008178	1098.025	31.97412	0.031275	0.011464	1096.023	38.46897	0.025995	0.012123	1098.023	34.27327	0.029177	0.010973
1098.022	32.08059	0.031172	0.009008	1100.024	52.20536	0.019155	0.015489	1098.021	38.55581	0.025936	0.01201	1100.021	54.84521	0.018233	0.010622
1100.024	52.52018	0.01904	0.009594	1102.024	56.82966	0.017596	0.016248	1100.021	59.01718	0.016944	0.012086	1102.021	59.17799	0.016898	0.010085
1102.024	56.89236	0.017577	0.010249	1104.024	56.9491	0.01756	0.015499	1102.021	63.06626	0.015856	0.012487	1104.021	59.23986	0.016881	0.00986
1104.024	57.02362	0.017537	0.010022	1106.024	56.94718	0.01756	0.016179	1104.021	63.20614	0.015821	0.012879	1106.023	59.13772	0.01691	0.010068
1106.024	56.96161	0.017556	0.009992	1108.024	56.81975	0.0176	0.015878	1106.024	63.24973	0.01581	0.011619	1108.021	59.03254	0.01694	0.010096
1108.023	56.86799	0.017585	0.010304	1110.025	74.01861	0.01351	0.019107	1108.022	63.04933	0.015861	0.011851	1110.022	76.54396	0.013064	0.012564
1110.024	74.21327	0.013475	0.014329	1112.024	77.30825	0.012935	0.019717	1110.024	80.33441	0.012448	0.013851	1112.022	79.77582	0.012535	0.012774
1112.024	77.33381	0.012931	0.015147	1114.024	77.30759	0.012935	0.019264	1112.023	83.94039	0.011913	0.014253	1114.023	79.84602	0.012524	0.012368
1114.024	77.46884	0.012908	0.014978	1116.024	77.39446	0.012921	0.019609	1114.022	83.80482	0.011932	0.014402	1116.021	79.68898	0.012549	0.012933
1116.023	77.33622	0.012931	0.014998	1118.024	77.4334	0.012914	0.019006	1116.021	83.73941	0.011942	0.014376	1118.022	79.59829	0.012563	0.012488
1118.024	77.44496	0.012912	0.015051	1120.024	51.77379	0.019315	0.015058	1118.022	83.95021	0.011912	0.014335	1120.021	54.45885	0.018362	0.009174
1120.023	51.90414	0.019266	0.010251	1122.023	45.77079	0.021848	0.014164	1122.022	52.5116	0.019043	0.009655	1122.021	48.35101	0.020682	0.008649
1122.025	45.91235	0.021781	0.008594	1124.025	45.91483	0.021779	0.013783	1124.022	52.5131	0.019043	0.009976	1124.022	48.16891	0.02076	0.00895
1124.023	46.06451	0.021709	0.007897	1126.025	45.7098	0.021877	0.013633	1124.022	52.5131	0.019043	0.009976	1126.022	48.163	0.020763	0.009174
1126.024	45.93012	0.021772	0.007751	1128.025	45.75532	0.021855	0.013707	1126.022	52.46635	0.01906	0.010114	1128.022	48.21784	0.020739	0.008473
1128.025	45.84454	0.021813	0.008452	1130.025	45.98594	0.021746	0.013704	1128.024	52.38923	0.019088	0.008883	1130.022	48.22422	0.020736	0.009746
1130.024	44.62562	0.022409	0.012558	1132.024	45.90616	0.021784	0.013692	1130.022	52.42221	0.019076	0.008837	1132.022	48.17904	0.020756	0.009322
1132.024	44.43664	0.022504	0.013308	1134.023	54.38881	0.018386	0.015497	1132.022	52.48615	0.019053	0.010132	1134.023	56.67894	0.017643	0.01013
1134.022	53.65042	0.018639	0.011446	1136.023	72.142	0.013862	0.018449	1134.022	60.78364	0.016452	0.01087	1136.021	74.30213	0.013459	0.012373
1136.024	71.38246	0.014009	0.012348	1138.023	72.16706	0.013857	0.018179	1136.021	78.72036	0.012703	0.01366	1138.022	74.23153	0.013471	0.011567
1138.023	71.16042	0.014053	0.011616	1140.024	72.05826	0.013878	0.018597	1138.022	78.73927	0.0127	0.013701	1140.023	74.1719	0.013482	0.012019
1140.024	70.9399	0.014096	0.01139	1142.024	72.14381	0.013861	0.018334	1140.022	78.71893	0.012703	0.013513	1142.021	74.29272	0.01346	0.011613
1142.024	71.64299	0.013958	0.012933	1144.025	89.55549	0.011166	0.022013	1142.023	78.67264	0.012711	0.013527	1144.023	99.85861	0.010014	0.015472
1144.023	90.50692	0.011049	0.017755	1146.025	141.0082	0.007092	0.028721	1144.022	109.635	0.009121	0.023631	1146.023	172.3281	0.005803	0.020211
1146.023	141.5645	0.007064	0.025889	1148.024	138.167	0.007238	0.028217	1146.023	187.8143	0.005324	0.034976	1148.022	171.3645	0.005836	0.01935
1148.026	143.9132	0.006949	0.026433	1150.024	139.9343	0.007146	0.028638	1148.022	187.8143	0.005324	0.034433	1150.022	172.5478	0.005795	0.01955
1150.023	141.4662	0.007069	0.026602	1152.024	136.9723	0.007301	0.028432	1150.023	187.8143	0.005324	0.034342	1152.022	173.8268	0.005753	0.019369
1152.025	142.98	0.006994	0.026681	1154.023	110.1662	0.009077	0.025145	1152.023	187.8143	0.005324	0.034894	1154.024	129.5349	0.00772	0.016995
1154.025	112.872	0.00886	0.023152	1156.024	70.70409	0.014143	0.017117	1154.022	145.2362	0.006885	0.028952	1156.022	73.20688	0.01366	0.010521
1156.023	70.7085	0.014143	0.013099	1158.024	70.81816	0.014121	0.017219	1156.022	77.97371	0.012825	0.012844	1158.023	73.11668	0.013677	0.010968
1158.024	70.69088	0.014146	0.012954	1160.025	70.56768	0.014171	0.017639	1158.023	77.91691	0.012834	0.012548	1160.023	73.10698	0.013679	0.010402
1160.023	70.79296	0.014126	0.013173	1162.025	70.61019	0.014162	0.017299	1160.022	77.77503	0.012858	0.012969	1162.023	73.28924	0.013645	0.010468
1162.024	70.82155	0.01412	0.012926	1164.024	62.70165	0.015949	0.01676	1162.023	77.96662	0.012826	0.012589	1164.022	65.26307	0.015323	0.010002
1164.023	62.82746	0.015917	0.011806	1166.023	45.70926	0.021877	0.014066	1164.023	69.97867	0.01429	0.011785	1166.021	48.44502	0.020642	0.008811
1166.024	45.57196	0.021943	0.008277	1168.025	45.69198	0.021886	0.013158	1166.022	52.4117	0.01908	0.010316	1168.024	48.19948	0.020747	0.008227
1168.023	45.86609	0.021803	0.007881	1170.025	45.73503	0.021865	0.014012	1168.023	52.59517	0.019013	0.009612	1170.023	48.33789	0.020688	0.008585
1170.023	45.68644	0.021888	0.008106	1172.025	45.77076	0.021848	0.013861	1170.022	52.65762	0.018991	0.009068	1172.024	48.29421	0.020706	0.008431
1172.024	45.5298	0.021964	0.008202	1174.026	45.78258	0.021842	0.013641	1172.023	52.70056	0.018975	0.010391	1174.022	48.15146	0.020768	0.00917
1174.024	45.88848	0.021792	0.008441	1176.025	45.67445	0.021894	0.013773	1174.023	52.5228	0.019039	0.009758	1176.023	48.24218	0.020729	0.008697
1176.023	45.86153	0.021805	0.007784	1178.026	45.73087	0.021867	0.013835	1176.024	52.52719	0.019038	0.010325	1178.023	48.29215	0.020707	0.009081
1178.024	45.77038	0.021848	0.00847	1180.026	71.22945	0.014039	0.018648	1178.023	52.62712	0.019002	0.00948	1180.024	73.39747	0.013624	0.012215
1180.024	71.17936	0.014049	0.013858	1182.026	77.26881	0.012942	0.019899	1180.025	77.84055	0.012847	0.014163	1182.023	79.59276	0.012564	0.012651
1182.025	77.14331	0.012963	0.015124	1184.025	77.37956	0.012923	0.019496	1182.023	83.80163	0.011933	0.014459	1184.021	79.73071	0.012542	0.012347
1184.024	77.19215	0.012955	0.015166	1186.023	77.42901	0.012915	0.019813	1184.023	83.79276	0.011934	0.014212	1186.022	79.68281	0.01255	0.012319
1186.023	77.2775	0.01294	0.015378	1188.024	77.25685	0.012944	0.019391	1186.023	83.78751	0.011935	0.0142	1188.022	79.60441	0.012562	0.012294
1188.025	77.14606	0.012962	0.014977	1190.024	58.65529	0.017049	0.016009	1188.024	83.75244	0.01194	0.014291	1190.023	61.08814	0.01637	0.00951
1190.025	58.95808	0.016961	0.011555	1192.024	55.17116	0.018125	0.015359	1190.024	65.6717	0.015227	0.011025	1192.023	57.66988	0.01734	0.008416
1192.024	55.2902	0.018086	0.009753	1194.023	55.19404	0.018118	0.015299	1192.023	62.14062	0.016093	0.011051	1194.025	57.6681	0.017341	0.008749
1194.024	55.18424	0.018121	0.009478	1196.025	55.20104	0.018116	0.015483	1194.024	62.11505	0.016099	0.011095	1196.023	57.72902	0.017322	0.008502
1196.023	55.2526	0.018099	0.009847	1198.024	55.28903	0.018087	0.015673	1196.023	62.23171	0.016069	0.011459	1198.023	57.60774	0.017359	0.00895
1198.023	55.2687	0.018093	0.009634	1200.024	36.17256	0.027645	0.012461	1198.023	62.20838	0.016075	0.011359	1200.024	38.00176	0.026315	0.009922
1200.023	36.12715	0.02768	0.009221	1202.026	31.9268	0.031322	0.011008	1200.022	42.7667	0.023383	0.011466	1202.023	34.2578	0.02919	0.010927
1202.024	31.8648	0.031383	0.008499	1204.026	31.93673	0.031312	0.011854	1202.024	38.35868	0.02607	0.012102	1204.023	34.32576	0.029133	0.00956
1204.023	31.77928	0.031467	0.008552	1206.023	31.99501	0.031255	0.011418	1204.022	38.4419	0.026013	0.011854	1206.023	34.15078	0.029282	0.009889

VLBT#	45			VLBT#	46			VLBT#	47			VLBT#	48		
SURFACE	**Carburized Ti-6Al-4V**			SURFACE	**Carburized Ti-6Al-4V**			SURFACE	**RMFC-4Z (Tiodize)**			SURFACE	**RMFC-4Z (Tiodize)**		
		Ave COF	**0.011**			Ave COF	**0.012**			Ave COF	**0.030**			Ave COF	**0.026**
		StdDev	**0.002**			StdDev	**0.003**			StdDev	**0.001**			StdDev	**0.003**
		Max COF	**0.017**			Max COF	**0.021**			Max COF	**0.033**			Max COF	**0.032**
		Min COF	0.009			Min COF	0.009			Min COF	0.028			Min COF	0.022
Time	Load, P	1/P	Fric Coeff	Time	Load, P	1/P	Fric Coeff	Time	Load, P	1/P	Fric Coeff	Time	Load, P	1/P	Fric Coeff
(s)	(N)	(N^-1)	(n/d)	(s)	(N)	(N^-1)	(n/d)	(s)	(N)	(N^-1)	(n/d)	(s)	(N)	(N^-1)	(n/d)
1080.015	55.26753	0.018094	0.009645	1080.023	55.24495	0.018101	0.010084	1082.018	31.11626	0.032138	0.030523	1082.02	30.96007	0.0323	0.023547
1082.016	35.88431	0.027867	0.010134	1082.021	35.98904	0.027786	0.010009	1084.019	31.16025	0.032092	0.032941	1084.02	31.05096	0.032205	0.022549
1084.015	31.80204	0.031445	0.010049	1084.021	31.96724	0.031282	0.01039	1086.02	31.13778	0.032115	0.032585	1086.019	30.98969	0.032269	0.022741
1086.016	31.80758	0.031439	0.011423	1086.023	31.84923	0.031398	0.010287	1088.018	31.21071	0.03204	0.031231	1088.019	30.85211	0.032413	0.023777
1088.014	31.88125	0.031366	0.010317	1088.023	31.86826	0.031379	0.010419	1090.019	31.12191	0.032132	0.032808	1090.01	30.91562	0.032346	0.023225
1090.016	31.991	0.031259	0.010837	1090.03	32.02627	0.031224	0.008652	1092.004	31.13704	0.032116	0.031837	1092.019	31.14389	0.032109	0.023025
1092.007	31.9008	0.031347	0.011294	1092.012	32.01626	0.031234	0.010931	1094.018	31.23146	0.032019	0.032	1094.018	31.00567	0.032252	0.02382
1094.031	31.89904	0.031349	0.011246	1094.022	32.09865	0.031154	0.009642	1096.018	31.15962	0.032093	0.032253	1096.018	31.20958	0.032041	0.022232
1096.016	31.88762	0.03136	0.010819	1096.022	31.89058	0.031357	0.009577	1098.018	31.13948	0.032114	0.031735	1098.017	31.1095	0.032145	0.023936
1098.015	31.91015	0.031338	0.010326	1098.022	31.89564	0.031352	0.010224	1100.03	31.16023	0.032092	0.032104	1100.017	51.49575	0.019419	0.026316
1100.016	31.87273	0.031375	0.010914	1100.038	32.06421	0.031187	0.010493	1102.019	51.65633	0.019359	0.030115	1102.018	55.80401	0.01792	0.025608
1102.015	52.56435	0.019024	0.010195	1102.023	52.64893	0.018994	0.011655	1104.019	55.89402	0.017891	0.030928	1104.018	55.96363	0.017869	0.026277
1104.016	56.87227	0.017583	0.010589	1104.021	56.87868	0.017581	0.012185	1106.018	55.9006	0.017889	0.029621	1106.02	55.91688	0.017884	0.025955
1106.017	56.77209	0.017614	0.010675	1106.022	56.75516	0.01762	0.011578	1108.019	55.94562	0.017874	0.030365	1108.019	55.95804	0.017871	0.025718
1108.028	56.86788	0.017585	0.010358	1108.022	56.85997	0.017587	0.011173	1110.018	55.84039	0.017908	0.030031	1110.018	73.13388	0.013674	0.028198
1110.014	57.07721	0.01752	0.010121	1110.022	56.89547	0.017576	0.011507	1112.018	73.25224	0.013651	0.030782	1112.019	76.48642	0.013074	0.02813
1112.041	74.24191	0.013469	0.012088	1112.022	74.45188	0.013431	0.01373	1114.019	76.50411	0.013071	0.030538	1114.02	76.60896	0.013053	0.028619
1114.016	77.45375	0.012911	0.012473	1114.023	77.44853	0.012912	0.013857	1116.02	76.61767	0.013052	0.030631	1116.02	76.33515	0.0131	0.028061
1116.015	77.34923	0.012928	0.012595	1116.022	77.51792	0.0129	0.014137	1118.019	76.63911	0.013048	0.030622	1118.018	76.38956	0.013091	0.02847
1118.021	77.2776	0.01294	0.012614	1118.021	77.48251	0.012906	0.013598	1120.018	76.34219	0.013099	0.030475	1120.018	50.9596	0.019623	0.025045
1120.015	77.39035	0.012922	0.012397	1122.021	51.84141	0.01929	0.010622	1122.017	50.60562	0.019761	0.029255	1122.019	44.64786	0.022397	0.024114
1122.017	51.82941	0.019294	0.009699	1124.022	45.67422	0.021894	0.009824	1124.018	44.83834	0.022302	0.029263	1124.018	44.83408	0.022304	0.023924
1124.017	45.74318	0.021861	0.009818	1126.021	45.81625	0.021826	0.00992	1126.018	44.85186	0.022296	0.030138	1126.021	44.75419	0.022344	0.023606
1126.031	45.62486	0.021918	0.009254	1128.022	45.84113	0.021814	0.009636	1128.018	44.9653	0.022239	0.02942	1128.019	44.69627	0.022373	0.024088
1128.014	45.70019	0.021882	0.008792	1130.023	45.90195	0.021786	0.009579	1130.018	44.83963	0.022302	0.029462	1130.019	44.99155	0.022226	0.024191
1130.015	45.72579	0.021869	0.010253	1132.021	45.65175	0.021905	0.009521	1132.019	44.8386	0.022302	0.029726	1134.018	53.16101	0.018811	0.02528
1132.015	45.68931	0.021887	0.009449	1134.021	45.7311	0.021867	0.010103	1134.02	44.90742	0.022268	0.030477	1136.018	71.12058	0.014061	0.027585
1134.017	45.62658	0.021917	0.00939	1136.022	54.43272	0.018371	0.011171	1136.019	53.83458	0.018575	0.029528	1138.036	71.02432	0.01408	0.027468
1136.031	53.89666	0.018554	0.011115	1138.022	72.12792	0.013864	0.013233	1138.018	71.39828	0.014006	0.030249	1140.018	71.17631	0.01405	0.027419
1138.015	72.12714	0.013864	0.011866	1140.021	72.10694	0.013868	0.013128	1140.018	71.38333	0.014009	0.030374	1142.02	71.09584	0.014066	0.02744
1140.017	72.26564	0.013838	0.012197	1142.023	72.14387	0.013861	0.013089	1142.019	71.36852	0.014012	0.030229	1144.02	81.87289	0.012214	0.028901
1142.015	71.98267	0.013892	0.012135	1144.023	72.24056	0.013843	0.013457	1144.018	71.1936	0.014046	0.030224	1146.02	103.8052	0.009633	0.031968
1144.016	72.15477	0.013859	0.012031	1146.021	86.77192	0.011524	0.015563	1146.019	82.55412	0.012113	0.03148	1148.019	104.9745	0.009526	0.032296
1146.015	86.44498	0.011568	0.014059	1148.023	126.6242	0.007897	0.020599	1148.018	105.4545	0.009483	0.03304	1150.02	103.7775	0.009636	0.032164
1148.014	127.5284	0.007841	0.017483	1150.023	128.2983	0.007794	0.020348	1150.018	106.1165	0.009424	0.032925	1152.018	104.6991	0.009551	0.032431
1150.025	125.9313	0.007941	0.017337	1152.044	128.1379	0.007804	0.020713	1152.02	106.6322	0.009378	0.033213	1154.02	92.3651	0.010827	0.030199
1152.031	125.9421	0.00794	0.017383	1154.023	125.4339	0.007972	0.020061	1154.02	104.8249	0.00954	0.032797	1156.019	69.79826	0.014327	0.02582
1154.015	126.1817	0.007925	0.017303	1156.02	105.7138	0.009459	0.017796	1156.019	92.07793	0.01086	0.031399	1158.019	69.6651	0.014354	0.026014
1156.025	102.8034	0.009727	0.015381	1158.021	70.77159	0.01413	0.011339	1158.019	69.71284	0.014345	0.02891	1160.02	69.73068	0.014341	0.026068
1158.017	70.48469	0.014187	0.011121	1160.022	70.61593	0.014161	0.011491	1160.019	69.86583	0.014313	0.028902	1162.019	69.71954	0.014343	0.02598
1160.017	70.63969	0.014156	0.01098	1162.019	70.60041	0.014164	0.011952	1162.02	69.9923	0.014287	0.02879	1164.02	61.71277	0.016204	0.025184
1162.016	70.62227	0.01416	0.010827	1164.023	70.68587	0.014147	0.011603	1164.018	69.82212	0.014322	0.029277	1166.019	44.64197	0.0224	0.022635
1164.016	70.70076	0.014144	0.010974	1166.024	62.62896	0.015967	0.011307	1166.019	61.70696	0.016206	0.028487	1168.019	44.55585	0.022444	0.022679
1166.017	62.57905	0.01598	0.010351	1168.043	45.6434	0.021909	0.009915	1168.02	44.7028	0.02237	0.029179	1170.018	44.6232	0.02241	0.022763
1168.017	45.48673	0.021984	0.008623	1170.022	45.67973	0.021892	0.009987	1170.02	44.73815	0.022352	0.028868	1172.018	44.78547	0.022329	0.022869
1170.015	45.51474	0.021971	0.009185	1172.032	45.53925	0.021959	0.008902	1172.038	44.65958	0.022392	0.029856	1174.018	44.60062	0.022421	0.023083
1172.016	45.40508	0.022024	0.009851	1174.022	45.74146	0.021862	0.009846	1174.044	44.60321	0.02242	0.029139	1176.019	44.83242	0.022305	0.02266
1174.016	45.64225	0.02191	0.009553	1176.021	45.8151	0.021827	0.009308	1176.02	44.7688	0.022337	0.028827	1178.02	44.66832	0.022387	0.023556
1176.034	45.51683	0.02197	0.008528	1178.022	45.5057	0.021975	0.009092	1178.018	44.79334	0.022325	0.029496	1180.02	70.42811	0.014199	0.02678
1178.015	45.52361	0.021967	0.009886	1180.022	45.52241	0.021967	0.009782	1180.018	44.91244	0.022266	0.028952	1182.02	76.41364	0.013087	0.027784
1180.015	45.67907	0.021892	0.009134	1182.023	71.23485	0.014038	0.01326	1182.036	70.46951	0.014191	0.029906	1184.019	76.21424	0.013121	0.027633
1182.016	71.24067	0.014037	0.011999	1184.023	77.05137	0.012978	0.013733	1184.019	76.35835	0.013096	0.030424	1186.02	76.42446	0.013085	0.027748
1184.014	77.22089	0.01295	0.012951	1186.022	76.95245	0.012995	0.013611	1186.022	76.30026	0.013106	0.030629	1188.022	76.14327	0.013133	0.027886
1186.017	77.23179	0.012948	0.01252	1188.023	77.03432	0.012981	0.01351	1188.02	76.34638	0.013098	0.030173	1190.018	57.78095	0.017307	0.024722
1188.017	77.30219	0.012936	0.013128	1190.023	77.08328	0.012973	0.013642	1190.02	76.30319	0.013106	0.030187	1192.018	54.57485	0.018323	0.023568
1190.014	77.26939	0.012942	0.012913	1192.022	58.71278	0.017032	0.010817	1192.021	57.72557	0.017323	0.028268	1194.02	54.72922	0.018272	0.024488
1192.017	58.48534	0.017098	0.009804	1194.023	55.21792	0.01811	0.010112	1194.019	54.67379	0.01829	0.028133	1196.019	54.72437	0.018273	0.023863
1194.015	55.11448	0.018144	0.009412	1196.021	55.0886	0.018153	0.00981	1196.02	54.5744	0.018324	0.028169	1198.019	54.57675	0.018323	0.023955
1196.016	55.1724	0.018125	0.010123	1198.032	55.15421	0.018131	0.010216	1198.019	54.64075	0.018301	0.028271	1200.019	35.02167	0.028554	0.022986
1198.035	55.22526	0.018108	0.009863	1200.022	55.2843	0.018088	0.009542	1200.018	54.63826	0.018302	0.028052	1202.02	30.85974	0.032405	0.022507
1200.028	55.06438	0.018161	0.009328	1202.022	35.51117	0.02816	0.010018	1202.019	34.93126	0.028628	0.031838	1204.02	30.97235	0.032287	0.021672
1202.016	35.88135	0.02787	0.010227	1204.023	31.72801	0.031518	0.010521	1204.021	31.01036	0.032247	0.032918	1206.019	30.90161	0.032361	0.022973
1204.017	31.85697	0.03139	0.010252	1206.023	31.93751	0.031311	0.010433	1206.02	31.19415	0.032057	0.033244				

VLBT#	**56**			VLBT#	**57**		
SURFACE	**HVPC ctg**			SURFACE	**HVPC ctg**		
		Ave COF	**0.006**			Ave COF	**0.007**
		StdDev	**0.001**			StdDev	**0.001**
		Max COF	**0.009**			Max COF	**0.010**
		Min COF	0.005			Min COF	0.005
Time	Load, P	1/P	Fric Coeff	Time	Load, P	1/P	Fric Coeff
(s)	(N)	(N^-1)	(n/d)	(s)	(N)	(N^-1)	(n/d)
1080.018	36.59672	0.027325	0.007628	1080.038	52.7898	0.018943	0.00599
1082.02	32.52089	0.030749	0.008367	1082.023	33.35009	0.029985	0.008509
1084.019	32.54778	0.030724	0.009075	1084.023	29.16408	0.034289	0.009736
1086.018	32.44983	0.030817	0.009461	1086.023	29.27072	0.034164	0.008915
1088.019	32.61433	0.030661	0.007948	1088.023	29.20188	0.034244	0.010386
1090.012	32.72129	0.030561	0.008387	1090.027	28.85204	0.03466	0.009779
1092.018	32.48682	0.030782	0.008974	1092.021	29.11294	0.034349	0.009906
1094.02	32.3891	0.030875	0.009435	1094.022	29.12649	0.034333	0.009488
1096.02	32.62658	0.03065	0.00814	1096.025	29.19542	0.034252	0.009823
1098.018	32.59324	0.030681	0.008936	1098.024	29.05468	0.034418	0.00981
1100.019	52.49177	0.019051	0.005379	1100.024	29.24297	0.034196	0.010028
1102.019	57.19178	0.017485	0.006475	1102.024	49.65892	0.020137	0.006568
1104.02	57.39909	0.017422	0.005817	1104.024	53.8656	0.018565	0.005329
1106.019	57.39645	0.017423	0.005777	1106.025	53.75651	0.018602	0.006568
1108.02	57.23058	0.017473	0.005842	1108.023	53.87547	0.018561	0.006195
1110.019	74.56093	0.013412	0.005211	1110.024	54.01417	0.018514	0.005911
1112.021	77.93781	0.012831	0.004968	1112.026	70.96283	0.014092	0.005751
1114.02	78.04081	0.012814	0.004831	1114.025	74.24463	0.013469	0.00568
1116.019	77.9418	0.01283	0.004833	1116.023	74.2062	0.013476	0.005657
1118.02	77.83656	0.012847	0.004798	1118.05	74.2248	0.013473	0.005937
1120.02	52.33795	0.019107	0.006297	1120.024	74.03972	0.013506	0.005662
1122.018	46.23881	0.021627	0.005923	1122.025	48.86575	0.020464	0.006694
1124.02	46.24986	0.021622	0.006952	1124.024	42.69431	0.023422	0.007843
1126.02	46.41315	0.021546	0.007274	1126.041	42.77433	0.023379	0.006367
1128.02	46.47353	0.021518	0.0066	1128.024	42.75452	0.023389	0.007491
1130.021	46.25534	0.021619	0.006596	1130.035	42.80486	0.023362	0.00692
1132.02	46.15851	0.021664	0.007128	1132.025	42.70912	0.023414	0.006749
1134.02	54.89241	0.018217	0.005689	1134.026	42.78291	0.023374	0.00733
1136.018	72.88418	0.01372	0.004934	1136.024	51.53756	0.019403	0.005843
1138.019	72.86142	0.013725	0.004919	1138.024	70.33978	0.014217	0.005616
1140.018	72.6834	0.013758	0.005037	1140.024	70.22564	0.01424	0.00626
1142.028	72.73747	0.013748	0.004927	1142.023	70.23124	0.014239	0.005734
1144.019	92.70528	0.010787	0.006127	1144.047	70.34443	0.014216	0.005575
1146.02	151.9346	0.006582	0.009036	1146.024	79.04606	0.012651	0.006454
1148.02	147.5769	0.006776	0.008632	1148.025	99.75572	0.010024	0.008124
1150.02	145.8858	0.006855	0.008338	1150.025	99.61036	0.010039	0.008068
1152.02	144.5056	0.00692	0.008318	1152.024	99.71847	0.010028	0.008261
1154.021	115.0827	0.008689	0.007611	1154.024	98.48012	0.010154	0.00813
1156.019	71.32516	0.01402	0.00491	1156.033	89.00965	0.011235	0.008099
1158.018	71.3862	0.014008	0.005135	1158.024	67.51138	0.014812	0.006116
1160.02	71.27737	0.01403	0.004804	1160.024	67.52659	0.014809	0.006538
1162.019	71.22741	0.01404	0.004792	1162.023	67.55021	0.014804	0.005679
1164.019	63.16135	0.015832	0.005566	1164.025	67.63496	0.014785	0.006074
1166.019	46.07235	0.021705	0.00649	1166.025	59.68869	0.016754	0.006194
1168.02	46.38382	0.021559	0.006488	1168.051	42.43852	0.023563	0.006896
1170.02	46.1538	0.021667	0.006771	1170.026	42.60934	0.023469	0.007145
1172.021	46.01582	0.021732	0.006643	1172.024	42.60449	0.023472	0.007455
1174.019	46.20325	0.021644	0.006204	1174.026	42.44182	0.023562	0.007492
1176.019	46.19986	0.021645	0.006979	1176.024	42.57499	0.023488	0.007245
1178.019	46.18061	0.021654	0.006951	1178.024	42.59539	0.023477	0.00717
1180.019	71.64799	0.013957	0.00458	1180.023	42.61189	0.023468	0.007225
1182.02	78.12119	0.012801	0.005185	1182.025	68.22145	0.014658	0.006463
1184.019	77.86873	0.012842	0.004885	1184.027	73.87462	0.013536	0.006115
1186.02	77.71049	0.012868	0.004667	1186.026	74.07531	0.0135	0.006394
1188.021	77.74742	0.012862	0.00516	1188.025	73.94401	0.013524	0.006277
1190.019	59.17474	0.016899	0.005837	1190.026	73.73637	0.013562	0.006157
1192.021	55.79567	0.017923	0.005479	1192.047	56.01297	0.017853	0.006804
1194.019	55.72421	0.017946	0.005756	1194.023	52.63402	0.018999	0.006584
1196.02	55.82434	0.017913	0.005618	1196.039	52.49492	0.019049	0.006071
1198.019	55.92169	0.017882	0.006273	1198.024	52.5735	0.019021	0.006609
1200.02	36.80502	0.02717	0.007357	1200.024	52.67965	0.018983	0.006463
1202.044	32.40931	0.030855	0.007696	1202.025	33.37196	0.029965	0.008879
1204.021	32.60882	0.030667	0.008388	1204.025	29.06504	0.034406	0.010192
1206.02	32.5196	0.030751	0.008463	1206.027	29.04917	0.034424	0.010674

Appendix C. Selected Properties of Cast Iron, Bronze, and Titanium Alloy

Property	Units	Gray Cast Iron*	Alloy 932 Bronze**	Ti64 (Grade 5)***
Nominal composition	wt%	3.4 – 3.7 wt% C, resid. S, P, O, Si, bal Fe.	83 Cu, 7.0 Pb, 6.9 Sn, 2.5 Zn, 0.35 Sb, 0.2 Fe, 1.0 Ni, minor Al, Si, S	5.5 – 6.8 Al, 3.5 – 4.5 V, 0.3 Fe, 0.2 O, 0.1 C, 0.05 N, ~ 0.01 H
Density	g/cm^3	7.2	8.91	4.42
Melting point	^oC		854	1650 - 1670
Elastic modulus	GPa	~ 200. – 211.	100.	107 – 122 (20 C) 105 – 111 (230 C)
Poissons ratio	(none)	0.17		0.31
Thermal conductivity	$W/m\text{-}^oK$	42 – 62	58.2 (20 C)	6.6 (20 C) 10.6 (315 C)
Specific heat	$J/(kg - ^oK)$	460.	377.	586. (20 – 570 C)
Coefficient of thermal expansion	$x\ 10^{-6} / ^oK$	8.1 – 19.3 (20 C)	18.0 (20-100 C)	9.0 (0 - 100 C) 9.4 (20 – 425 C)

Table references:

* R. L. Hecht, R. B. Dinwiddie, W. D. Porter, and H. Wang (1996) "Thermal Transport Properties of Grey Cast Irons," Soc. of Automotive Engineers, paper number 962126.

** Atlas Bronze website, www.atlasbronze.com, on-line data table (2012).

*** TIMET Corporation, Denver, CO, on-line alloy data sheets (2002).

List of Figures

Figure **Page**

List of Tables

Table **Page**